

# A Nonlinear Moment Model for Radiative Transfer Equation

Ruo Li\*, Peng Song<sup>†</sup> and Lingchao Zheng<sup>‡</sup>

May 28, 2020

## Abstract

We derive a nonlinear moment model for radiative transfer equation in 3D space, using the method to derive the nonlinear moment model for the radiative transfer equation in slab geometry. The resulted 3D  $HMP_N$  model enjoys a list of mathematical advantages, including global hyperbolicity, rotational invariance, physical wave speeds, spectral accuracy, and correct higher-order Eddington approximation. Simulation examples are presented to validate the new model numerically.

**Keywords:** Radiative transfer equation; moment method; nonlinear model; global hyperbolicity.

## 1 Introduction

The radiative transfer equation (RTE) depicts the motion of photons and their interaction with the background medium. It has lots of applications, such as radiation astronomy [35], optical imaging [26, 40], neutron transport in reactor physics [37, 16], light transport in atmospheric radiative transfer [31] and heat transfer [27]. Due to the integro-differential form and the high-dimensionality of RTE, how to develop efficient methods to solve it numerically is an important but challenging topic. So far, the commonly used numerical methods can be categorized into two groups: the probabilistic methods, like the direct simulation Monte Carlo (DSMC) method [21, 3, 24, 14, 1], and the deterministic methods [4, 28, 39, 25, 13, 15, 36, 2, 17, 20, 19], such as the discrete ordinates method ( $S_N$ ) [4, 28, 39], the moment methods [25, 13, 15, 2, 20, 19] and etc.

The discrete ordinates method ( $S_N$ ) is one of the most popular numerical methods to simulate the RTE, which solve the RTE along with a discrete set of angular directions from a given quadrature set. However, the  $S_N$  model assumes that the particles can only move along the directions in the quadrature set, thus once the coordinate system is rotated, the results of the  $S_N$  model can be different. The lack of rotational invariance results in numerical artifacts, known as *ray effects* [28].

In order to reduce the complexity of the RTE, the moment method focuses on the evolution of a finite number of moments of the specific intensity, which avoids the high-dimensionality of directly solving the RTE. Since the governing equation of a lower order moment commonly contains higher order moments, the moment system is often not automatically closed. Hence one has to take a *moment closure* to close the moment system. A practical method for the moment closure is to construct an ansatz to approximate the specific intensity. The pioneer works in moment method include the spherical harmonics method ( $P_N$ ) [37] and the maximum entropy method ( $M_N$ ) [29, 15, 36]. The  $P_N$  model constructs the ansatz using spherical harmonic polynomials. It can be regarded as a polynomial expansion of the specific intensity around the equilibrium, which is a constant function. One of the flaws is that the resulting system may lead to nonphysical oscillations, or even worse, negative particle concentration [6, 7, 34]. The  $M_N$  model constructs the ansatz using the principle of maximum entropy, as the maximum entropy closure for Boltzmann equation [29, 15]. Unfortunately, no explicit expression of the moment closure for  $M_N$  model can be given when the order  $N \geq 2$ . To implement the model numerically, one has to solve an ill-conditioned optimization problem to obtain an approximate moment closure. This almost prohibits the application of the  $M_N$  model.

Recently, a nonlinear moment model (called the  $MP_N$  model) was proposed in [20] for the RTE in slab geometry. This model takes the ansatz of the  $M_1$  model (the first order  $M_N$  model) as the weight function, then constructs the ansatz by expanding the specific intensity around the weight function in

\*CAPT, LMAM & School of Mathematical Sciences, Peking University, Beijing, China, email: rli@math.pku.edu.cn

<sup>†</sup>Institute of Applied Physics and Computational Mathematics, Beijing, China, email: song\_peng@iapcm.ac.cn

<sup>‡</sup>School of Mathematical Sciences, Peking University, Beijing, China, email: lczheng@pku.edu.cn

terms of orthogonal polynomials in the velocity variables. Numerical examples in [20] demonstrated a quite promising performance as an improved approximation of the intensity in comparison of the  $P_N$  model. The  $MP_N$  model was further improved in [19] by a globally hyperbolic regularization following the framework developed in [8, 9, 10, 18]. We note that the regularization in [19] is a subtle modification of the work in [10] instead of a direct application. Otherwise, the resulting system may change the  $M_1$  model, which leads to a wrong higher-order Eddington approximation. Eventually, the  $HMP_N$  model was proposed in [19] with not only global hyperbolicity, but also a physical higher-order Eddington approximation.

Encouraged by the elegant mathematical structure and the promising numerical performance of the  $HMP_N$  model for RTE in slab geometry, we in this paper try to extend the method to derive the  $HMP_N$  model for 3D problems. The steps of the extension are clear while there are still numerous difficulties. Fortunately, the 3D  $M_1$  model is explicit, which allow us to construct the ansatz to approximate the specific intensity using again the weighted polynomials with the weight function is the ansatz of the  $M_1$  model. To construct the function space of the weighted polynomials, we need to give the orthogonal polynomial basis with respect to the weight function. For the slab geometry [20], this can be implemented by a simple Gram-Schmidt orthogonalization. For the 3D case, we have to use quasi-orthogonal polynomials rather than orthogonal polynomials. Otherwise, it can be extremely involving to accomplish the calculation, which makes further analysis to the resulted model prohibited. We propose a procedure to make a quasi Gram-Schmidt orthogonalization to obtain the quasi-orthogonal polynomials in explicit expressions. This provides us a 3D  $MP_N$  model in explicit formation, which can be mathematically analyzed. To achieve global hyperbolicity, we still adopt the method in [19] to regularize the 3D  $MP_N$  model. Quite smoothly a globally hyperbolic 3D  $HMP_N$  model is eventually attained with a list of fabulous mathematical natures inherited from its 1D counterpart for the slab geometry. The resulted model is rotational invariant, with wave speeds not greater than that of light, spectral approximation accuracy, and correct higher-order Eddington approximation. We carry out preliminary numerical simulating using an abruptly splitting scheme to validate the new 3D  $HMP_N$  model. Some numerical examples on typical problems are presented with satisfactory performance.

The rest of this paper is arranged as follows. In Section 2, we briefly introduce the moment methods for RTE, and review how the  $MP_N$  and the  $HMP_N$  model in slab geometry were derived in [20, 19]. In Section 3, we derive the 3D  $MP_N$  model and prove that the model is rotational invariant. The hyperbolic regularization is applied to give the  $HMP_N$  model in Section 4. The model is analyzed in detail therein. In Section 5, we introduce the numerical scheme to carry out numerical simulations and present some numerical examples. The paper is then ended with a short conclusion remarks.

## 2 Preliminary

To model radiative transfer, the governing equation is a time-dependent equation of the *specific intensity*  $I$  as

$$\frac{1}{c} \frac{\partial I}{\partial t} + \boldsymbol{\Omega} \cdot \nabla_{\mathbf{x}} I = \mathcal{S}(I), \quad (2.1)$$

where  $c$  is the speed of light, and the specific intensity  $I = I(t, \mathbf{x}; \boldsymbol{\Omega}, \nu)$  depends on time  $t \in \mathbb{R}^+$ , the spatial coordinate of the photon  $\mathbf{x} \in \mathbb{R}^3$ , the velocity direction  $\boldsymbol{\Omega} \in \mathbb{S}^2$  and the frequency  $\nu \in \mathbb{R}^+$ . In this paper, our study omits the independent variable  $\nu$  that  $I$  is a function of  $t$ ,  $\mathbf{x}$  and  $\boldsymbol{\Omega}$  only. The right hand side  $\mathcal{S}(I)$  denotes the actions by the background medium on the photons. A form of  $\mathcal{S}(I)$  adopted commonly was given in [5, 33] as

$$\mathcal{S}(I) = -\sigma_t I + \frac{1}{4\pi} a c \sigma_a T^4 + \frac{1}{4\pi} \sigma_s \int_{\mathbb{S}^2} I d\boldsymbol{\Omega} + \frac{s}{4\pi}, \quad (2.2)$$

where  $a$  is the radiation constant, and  $s = s(t, \mathbf{x})$  is an isotropic external source of radiation. The scattering coefficient  $\sigma_s$ , the absorption coefficient  $\sigma_a$ , and the material temperature  $T(t, \mathbf{x})$  depend on time  $t$  and the spatial position  $\mathbf{x}$ . The total opacity coefficient is  $\sigma_t = \sigma_a + \sigma_s$ .

In case that the problems slab geometry and spherical symmetric geometry are considered, the 3D RTE (2.1) can be simplified to 1D problem. Precisely, in the slab geometry, the specific intensity depends only upon the single spatial coordinate  $z$  and the single angular coordinate  $\arccos \mu$ , the angle between  $\boldsymbol{\Omega}$  and the  $z$ -axis. Then the specific intensity becomes  $I = I(z, \mu)$ , and (2.1) is simplified as

$$\frac{1}{c} \frac{\partial I}{\partial t} + \mu \frac{\partial I}{\partial z} = \mathcal{S}(I). \quad (2.3)$$

The spherical geometry with perfect symmetry is a slightly more complicated case. The RTE, where the specific intensity depends upon only on the distance from the origin  $r = \|\mathbf{x}\|$ , and the angular variable  $\arccos \mu$ , which is the angle between  $\mathbf{\Omega}$  and  $\mathbf{x}$ . In this case,  $I = I(r, \mu)$ , and the 3D RTE (2.1) is simplified as

$$\frac{1}{c} \frac{\partial I}{\partial t} + \mu \frac{\partial I}{\partial r} + \frac{1 - \mu^2}{r} \frac{\partial I}{\partial \mu} = \mathcal{S}(I). \quad (2.4)$$

In [2, 20, 19, 30], for slab geometry and spherical symmetric geometry, some nonlinear moment models had been derived with global hyperbolicity and promising performance in handling problems with fair extreme specific intensity functions. The major aim of this paper is to develop models for 3D problems with similar techniques.

At first, we define the moments of the 3D specific intensity. Let  $\alpha \in \mathbb{N}^3$  be a 3D multi-index, i.e.  $\alpha = (\alpha_1, \alpha_2, \alpha_3)^T$ ,  $\alpha_1, \alpha_2, \alpha_3 \in \mathbb{N}$ . We define a function of  $t$ , and  $\mathbf{x}$ , denoted by  $\langle I \rangle_\alpha(t, \mathbf{x})$ , as

$$\langle I \rangle_\alpha(t, \mathbf{x}) \triangleq \int_{\mathbb{S}^2} \mathbf{\Omega}^\alpha I(t, \mathbf{x}; \mathbf{\Omega}) d\mathbf{\Omega}, \quad \alpha \in \mathbb{N}^3, \quad (2.5)$$

where  $\mathbf{\Omega}^\alpha = \Omega_1^{\alpha_1} \Omega_2^{\alpha_2} \Omega_3^{\alpha_3}$ . We call that  $\langle I \rangle_\alpha$  is the  $\alpha$ -th moment of the specific intensity  $I$ .

Notice that  $\mathbf{\Omega} \in \mathbb{S}^2$  implies  $\|\mathbf{\Omega}\| = 1$ , thus one has

$$\sum_{d=1}^3 \langle I \rangle_{\alpha+2e_d} = \langle I \rangle_\alpha, \quad \forall \alpha \in \mathbb{N}^3,$$

where  $e_d$  represents the multi-index whose  $d$ -th index is 1, and the else two indexes are 0. Therefore, we only need to consider these moments  $\langle I \rangle_\alpha$ ,  $\alpha \in \mathcal{I}$ , where  $\mathcal{I}$  is a set of multi-indexes, defined by

$$\mathcal{I} \triangleq \{\alpha : \alpha \in \mathbb{N}^3, \alpha_3 \leq 1\}. \quad (2.6)$$

The *order of the multi-index*  $\alpha$  is defined as  $|\alpha| = \sum_{d=1}^3 \alpha_d$ , and we denote that  $\mathcal{I}_N \triangleq \{\alpha : \alpha \in \mathcal{I}, |\alpha| \leq N\}$ . It is clear that once  $\{\langle I \rangle_\alpha : \alpha \in \mathcal{I}_N\}$  is determined, one can obtain  $\{\langle I \rangle_\alpha : \alpha \in \mathbb{N}^3, |\alpha| \leq N\}$ . This allows us to discuss  $\langle I \rangle_\alpha$  for  $\alpha \in \mathcal{I}$  only to derive reduced models.

Multiplying (2.1) by  $\mathbf{\Omega}^\alpha$ , and taking the integration with respect to  $\mathbf{\Omega}$  over  $\mathbb{S}^2$ , one can have

$$\frac{1}{c} \frac{\partial \langle I \rangle_\alpha}{\partial t} + \sum_{d=1}^3 \frac{\partial \langle I \rangle_{\alpha+e_d}}{\partial x_d} = \langle \mathcal{S}(I) \rangle_\alpha, \quad \alpha \in \mathcal{I}. \quad (2.7)$$

In order to derive a moment model for (2.1), we first truncate the system by discarding all the governing equations of high order moments  $\langle I \rangle_\alpha$ , where  $|\alpha| > N$ , for a given integer  $N \in \mathbb{N}$ . The truncated moment system is

$$\frac{1}{c} \frac{\partial \langle I \rangle_\alpha}{\partial t} + \sum_{d=1}^3 \frac{\partial \langle I \rangle_{\alpha+e_d}}{\partial x_d} = \langle \mathcal{S}(I) \rangle_\alpha, \quad \alpha \in \mathcal{I}_N. \quad (2.8)$$

However, the governing equations of  $\langle I \rangle_\alpha$ ,  $|\alpha| = N$ , involve three  $N + 1$  order moments  $\langle I \rangle_{\alpha+e_d}$  for  $d = 1, 2, 3$ , thus the truncated system (2.8) is not closed. Therefore, we need to determine all these moments,  $\{\langle I \rangle_\alpha, \alpha \in \mathcal{I}_{N+1}\}$  to make this truncated system (2.8) closed.

We divide the moments in  $\{\langle I \rangle_\alpha, \alpha \in \mathcal{I}_{N+1}\}$  into two parts: lower-order moments (also referred as *known moments* later on), and higher-order moments (also referred as *unknown moments* later on).

$$\begin{array}{ccc} \langle I \rangle_\alpha, \alpha \in \mathcal{I}_{N+1}, |\alpha| \leq N & & \langle I \rangle_\alpha, \alpha \in \mathcal{I}_{N+1}, |\alpha| = N + 1 \\ \Downarrow & & \Downarrow \\ \text{lower-order moments} & & \text{higher-order moments} \\ \text{(known moments)} & & \text{(unknown moments)} \end{array} \quad (2.9)$$

The aim of the so-called *moment closure* to this system is to approximate the unknown moments as functions of known moments, saying to give a formulation as

$$\langle I \rangle_\alpha \approx E_\alpha = E_\alpha(\langle I \rangle_\beta, \beta \in \mathcal{I}_N), \quad \text{for } \alpha \in \mathcal{I}_{N+1}, |\alpha| = N + 1. \quad (2.10)$$

To achieve this goal, a practical approach is to construct an ansatz for the specific intensity. Precisely, let  $E_\alpha$ ,  $\alpha \in \mathcal{I}_N$ , be the known moments for a certain unknown specific intensity  $I$ . Then one may propose an expression  $\hat{I}(\boldsymbol{\Omega}; E_\alpha, \alpha \in \mathcal{I}_N)$ , called an *ansatz* to approximate  $I$ , such that

$$\langle \hat{I}(\cdot; E_\alpha, \alpha \in \mathcal{I}_N) \rangle_\alpha = E_\alpha, \quad \alpha \in \mathcal{I}_N. \quad (2.11)$$

Often we require that  $\hat{I}$  is uniquely determined by the consistency relations (2.11). With  $\hat{I}$  given, the higher-order moments of  $I$  are then approximated by the higher-order moments of  $\hat{I}$ , i.e.,

$$E_\alpha = \langle \hat{I}(\cdot; E_\beta, \beta \in \mathcal{I}_N) \rangle_\alpha, \quad \alpha \in \mathcal{I}_{N+1}, |\alpha| = N+1. \quad (2.12)$$

Therefore, one may take the closed moment system

$$\frac{1}{c} \frac{\partial E_\alpha}{\partial t} + \sum_{d=1}^3 \frac{\partial E_{\alpha+e_d}}{\partial x_d} = \langle \mathcal{S}(\hat{I}) \rangle_\alpha, \quad \alpha \in \mathcal{I}_N, \quad (2.13)$$

as the reduced model to approximate the original RTE, where  $E_{\alpha+e_d}$  are functions of  $E_\alpha$ ,  $\alpha \in \mathcal{I}_N$ , defined in (2.10) and (2.12).

Many existing models can be regarded as consequences using this moment closure approach. For example, the  $P_N$  model [25], the  $M_N$  model [29, 15], the positive  $P_N$  model [22], the  $B_2$  model [2], and the  $MP_N$  model [20] are in this fold. The  $MP_N$  model we proposed in [20], and then improved in [19] as the  $HMP_N$  model, is limited for problems in slab geometry, where it exhibits satisfactory numerical performance for some standard benchmarks. To extend the method therein to 3D RTE, below we first briefly review the methods in [20, 19] to derive models in slab geometry to clarify our idea.

The  $MP_N$  model derived in [20] for RTE in slab geometry is based on a method to combine the  $P_N$  model and the  $M_N$  model, which was implemented by expanding the specific intensity around the ansatz of the  $M_1$  model in terms of orthogonal polynomials. The ansatz of the  $M_1$  model in slab geometry is

$$\hat{I}_{M_1} = \frac{\varepsilon}{(1 + c_0 \mu)^4}, \quad (2.14)$$

where  $\varepsilon$  and  $c_0$  are determined by the 0-th moment  $E_0$  and 1-th moment  $E_1$ , formulated as

$$c_0 = -\frac{3E_1/E_0}{2 + \sqrt{4 - 3(E_1/E_0)^2}}, \quad \varepsilon = \frac{3(1 - c_0^2)^3}{2(3 + c_0^2)}. \quad (2.15)$$

Then the specific intensity is approximated by a weighted polynomial, with the weight function

$$\omega^{[c_0]}(\mu) = \frac{1}{(1 + c_0 \mu)^4}. \quad (2.16)$$

The function space of the weighted polynomials is

$$\mathbb{H}_N^{[c_0]} \triangleq \left\{ \omega^{[c_0]} \sum_{k=0}^N g_k \mu^k \right\}. \quad (2.17)$$

Then the ansatz of the  $MP_N$  model is written as

$$\hat{I}(\mu; E_0, \dots, E_N) \triangleq \sum_{i=0}^N f_i \Phi_i^{[c_0]}(\mu) \in \mathbb{H}_N^{[c_0]}, \quad \Phi_i^{[c_0]}(\mu) = \phi_i^{[c_0]}(\mu) \omega^{[c_0]}(\mu), \quad (2.18)$$

where  $\Phi_i^{[c_0]}(\mu) = \phi_i^{[c_0]}(\mu) \omega^{[c_0]}(\mu)$ ,  $i = 0, 1, \dots, N$ , are the basis functions,  $\phi_i^{[c_0]}(\mu)$  are orthogonal polynomials with respect to the weight function, and  $f_i$  are the expansion coefficients.

The orthogonal polynomials  $\phi_k^{[c_0]}(\mu)$  can be calculated by a simple Gram-Schmidt orthogonalization, formulated as

$$\phi_0^{[c_0]}(\mu) = 1, \quad \phi_j^{[c_0]}(\mu) = \mu^j - \sum_{k=0}^{j-1} \frac{\mathcal{K}_{j,k}}{\mathcal{K}_{k,k}} \phi_k^{[c_0]}(\mu), \quad j \geq 1, \quad (2.19)$$

where  $\mathcal{K}_{j,k} = \int_{-1}^1 \mu^j \phi_k^{[c_0]}(\mu) \omega^{[c_0]}(\mu) d\mu$ , calculated by

$$\mathcal{K}_{0,0} = \langle \omega^{[c_0]}(\mu) \rangle_0, \quad \mathcal{K}_{i,j} = \langle \omega^{[c_0]}(\mu) \rangle_{i+j} - \sum_{k=0}^{j-1} \frac{\mathcal{K}_{j,k} \mathcal{K}_{i,k}}{\mathcal{K}_{k,k}}, \quad 1 \leq j \leq i. \quad (2.20)$$

Furthermore, by

$$f_0 = \frac{E_0}{\mathcal{K}_{0,0}}, \quad f_i = \frac{1}{\mathcal{K}_{i,i}} \left( E_i - \sum_{j=0}^{i-1} \mathcal{K}_{i,j} f_j \right), \quad 1 \leq i \leq N, \quad (2.21)$$

one can determine the coefficients  $f_k$ , and the ansatz  $\hat{I}(\mu; E_0, E_1, \dots, E_N)$ . Finally, we have the moment closure as

$$E_{N+1} = \sum_{k=0}^N f_k \mathcal{K}_{N+1,k}. \quad (2.22)$$

Meanwhile, in the viewpoint of orthogonal projection, if we define the orthogonal projection to function space  $\mathbb{H}_N^{[c_0]}$ ,

$$\mathcal{P}_N : f = \sum_{k=0}^{+\infty} f_k \Phi_k^{[c_0]}(\mu) \rightarrow \mathcal{P}_N f = \sum_{k=0}^N f_k \Phi_k^{[c_0]}(\mu), \quad (2.23)$$

then the  $MP_N$  moment system can be written as

$$\frac{1}{c} \mathcal{P}_N \frac{\partial \mathcal{P}_N I}{\partial t} + \mathcal{P}_N \mu \frac{\partial \mathcal{P}_N I}{\partial z} = \mathcal{P}_N \mathcal{S}(\mathcal{P}_N I). \quad (2.24)$$

The weight function (2.16) permits the  $MP_N$  model to approximate a strongly anisotropic distribution with very high accuracy. In [19], the  $MP_N$  model was further improved by a hyperbolic regularization, which provides global hyperbolicity. To achieve the required hyperbolicity, the model reduction framework in [10, 18] suggests adding one more projection between the operators  $\mu \cdot$  and  $\frac{\partial \cdot}{\partial z}$  in (2.24) to regularize the  $MP_N$  model to be globally hyperbolic, and the resulting model is

$$\frac{1}{c} \mathcal{P}_N \frac{\partial \mathcal{P}_N I}{\partial t} + \mathcal{P}_N \mu \mathcal{P}_N \frac{\partial \mathcal{P}_N I}{\partial z} = \mathcal{P}_N \mathcal{S}(\mathcal{P}_N I). \quad (2.25)$$

An interesting point observed in [19] is that this regularization changes the  $MP_N$  model when  $N = 1$ . It is definitely inappropriate that the  $M_1$  model is changed by the regularization. In order to fix this defect, another weight function is introduced as

$$\tilde{\omega}^{[c_0]} = \frac{1}{(1 + c_0 \mu)^5}, \quad (2.26)$$

and then a new function space is defined as

$$\tilde{\mathbb{H}}_N^{[c_0]} \triangleq \left\{ \tilde{\omega}^{[c_0]} \sum_{k=0}^N g_k \mu^k \right\}. \quad (2.27)$$

In this subspace, one can define the orthogonal polynomials  $\tilde{\phi}_k^{[c_0]}(\mu)$  and the basis function  $\tilde{\Phi}_k^{[c_0]}(\mu)$ ,  $0 \leq k \leq N$ . Furthermore, a new projection  $\tilde{\mathcal{P}}_N$  is defined as

$$\tilde{\mathcal{P}}_N : f = \sum_{k=0}^{+\infty} f_k \tilde{\Phi}_k^{[c_0]}(\mu) \rightarrow \tilde{\mathcal{P}}_N f = \sum_{k=0}^N f_k \tilde{\Phi}_k^{[c_0]}(\mu). \quad (2.28)$$

The new hyperbolic regularization in [19] adds one more projection  $\tilde{\mathcal{P}}_N$  to give the  $HMP_N$  model formulated as

$$\frac{1}{c} \tilde{\mathcal{P}}_N \frac{\partial \mathcal{P}_N I}{\partial t} + \tilde{\mathcal{P}}_N \mu \tilde{\mathcal{P}}_N \frac{\partial \mathcal{P}_N I}{\partial z} = \tilde{\mathcal{P}}_N \mathcal{S}(\mathcal{P}_N I). \quad (2.29)$$

It was revealed that the  $HMP_N$  model enjoys some desired properties, such as

**Property 1.** 1. The  $HMP_N$  model is globally hyperbolic.

2. The characteristic speeds of the  $HMP_N$  model lie in  $[-c, c]$ .

3. The regularization vanishes for the case  $N = 1$ .

4. Between the  $MP_N$  model and the  $HMP_N$  model, the governing equation of  $E_k$ ,  $k = 0, \dots, N - 1$  is not changed.

### 3 Moment Model Reduction

In this section, we adopt the strategy introduced in Section 2 to derive a  $MP_N$  type model for the 3D RTE at first.

#### 3.1 Formal derivation

Let us start with the  $M_1$  model in 3D case. The ansatz of specific intensity is

$$\hat{I}_{M_1}(\mathbf{\Omega}; E_0, E_{e_1}, E_{e_2}, E_{e_3}) = \frac{\varepsilon}{(1 + \mathbf{c}_0 \cdot \mathbf{\Omega})^4}. \quad (3.1)$$

with the known moments  $E_0, E_{e_1}, E_{e_2},$  and  $E_{e_3}$ . We denote them as  $\mathbf{E}_0 = (E_0)^T$ , and  $\mathbf{E}_1 = (E_{e_1}, E_{e_2}, E_{e_3})^T$ , respectively. Direct calculation yields that

$$\mathbf{c}_0 = \frac{-2 + \sqrt{4 - 3(\|\mathbf{E}_1\|/E_0)^2}}{\|\mathbf{E}_1\|/E_0} \frac{\mathbf{E}_1}{\|\mathbf{E}_1\|}, \quad (3.2)$$

Following [20], we approximate the specific intensity with a weighted polynomial, and the weight function is chosen as the ansatz of the  $M_1$  model, as (3.1). For simplicity, we take the weight function as

$$\omega^{[c_0]}(\mathbf{\Omega}) = \frac{1}{(1 + \mathbf{c}_0 \cdot \mathbf{\Omega})^4}.$$

Then the function space of weighted polynomials is defined as

$$\mathbb{H}_N^{[c_0]} \triangleq \left\{ \omega^{[c_0]}(\mathbf{\Omega}) \sum_{\alpha \in \mathcal{I}_N} g_\alpha \mathbf{\Omega}^\alpha \right\}. \quad (3.3)$$

The ansatz of the 3D  $MP_N$  model  $\hat{I}(\mathbf{\Omega})$  is chosen to satisfy

$$\hat{I} \in \mathbb{H}_N^{[c_0]}, \quad \langle \hat{I} \rangle_\alpha = E_\alpha, \quad \alpha \in \mathcal{I}_N.$$

In order to determine the ansatz  $\hat{I}$ , we first rewrite  $\hat{I}$  as

$$\hat{I}(t, \mathbf{x}; \mathbf{\Omega}) = \hat{I}(t; \mathbf{E}) = \sum_{\alpha \in \mathcal{I}_N} f_\alpha(t, \mathbf{x}) \phi_\alpha^{[c_0]}(\mathbf{\Omega}) \omega^{[c_0(t, \mathbf{x})]}(\mathbf{\Omega}) \in \mathbb{H}_N^{[c_0]}, \quad (3.4)$$

where  $\phi_\alpha^{[c_0]}, \alpha \in \mathcal{I}_N$  are quasi-orthogonal polynomials with respect to the weight function  $\omega^{[c_0]}$ , and  $f_\alpha$  are the corresponding coefficients. On the quasi-orthogonal polynomials, we define the inner product

$$\langle f, g \rangle_{\mathbb{H}_N^{[c_0]}} \triangleq \int_{\mathbb{S}^2} f g \omega^{[c_0]} d\mathbf{\Omega}, \quad (3.5)$$

then the quasi-orthogonal polynomials  $\phi_\alpha^{[c_0]}$  satisfy that

$$\left\langle \phi_\alpha^{[c_0]}, \phi_\beta^{[c_0]} \right\rangle_{\mathbb{H}_N^{[c_0]}} = \int_{\mathbb{S}^2} \phi_\alpha^{[c_0]}(\mathbf{\Omega}) \phi_\beta^{[c_0]}(\mathbf{\Omega}) \omega^{[c_0]}(\mathbf{\Omega}) d\mathbf{\Omega} = 0, \quad \text{when } |\alpha| \neq |\beta|. \quad (3.6)$$

Moreover, the quasi-polynomial  $\phi_\alpha^{[c_0]}$  satisfies that its only  $|\alpha|$ -order term is  $\mathbf{\Omega}^\alpha$ , i.e.

$$\phi_\alpha^{[c_0]} = \mathbf{\Omega}^\alpha + \sum_{\beta \in \mathcal{I}_{|\alpha|-1}} h_{\alpha, \beta} \mathbf{\Omega}^\beta. \quad (3.7)$$

For later usage, we denote the quasi-orthogonal functions

$$\Phi_\alpha^{[c_0]} = \phi_\alpha^{[c_0]} \omega^{[c_0]}. \quad (3.8)$$

**Remark 1.** Let us remark that  $\phi_\alpha^{[c_0]}, \alpha \in \mathcal{I}$  are quasi-orthogonal polynomials, rather than orthogonal polynomials. In other words,  $\left\langle \phi_\alpha^{[c_0]}, \phi_\beta^{[c_0]} \right\rangle_{\mathbb{H}_N^{[c_0]}}$  can be non-zero for  $|\alpha| = |\beta|$  and  $\alpha \neq \beta$ .

Let us construct these quasi-orthogonal polynomials  $\phi_\alpha^{[c_0]}$  by the Gram-Schmidt orthogonalization. This Gram-Schmidt orthogonalization is different from the 1D case used in [20]. We denote  $\mathcal{E}_\alpha$  as the moments of the weight function  $\mathcal{E}_\alpha \triangleq \langle \omega^{[c_0]} \rangle_\alpha$  for later usage.

In (3.2), we denote  $\mathbf{E}_0$  and  $\mathbf{E}_1$  as the vector of moments of order 0 and order 1. In the following discussion, we will continue to use this notation, i.e. we denote  $\mathbf{E}_k$  as the vector of moments of order  $k$ , whose dimension is  $2k + 1$ . Similarly, we can denote  $\phi_k^{[c_0]}$ ,  $\Phi_k^{[c_0]}$ ,  $\mathbf{f}_k$  and  $\mathcal{E}_k$ . Using this notation, the moment closure

$$E_\alpha(E_\beta, \beta \in \mathcal{I}_N), \quad |\alpha| = N + 1, \alpha \in \mathcal{I}$$

can be rewritten as

$$\mathbf{E}_{N+1}(\mathbf{E}_k, 0 \leq k \leq N).$$

We denote by  $\varphi_k$  to be the vector of  $\Omega^\alpha$ ,  $\alpha \in \mathcal{I}$  and  $|\alpha| = k$ . Using these notations, the ansatz (3.4) is rewritten as

$$\hat{I} = \sum_{k=0}^N \mathbf{f}_k \Phi_k^{[c_0]} = \omega^{[c_0]} \sum_{k=0}^N \mathbf{f}_k \phi_k^{[c_0]}. \quad (3.9)$$

We denote the inner product as

$$\mathcal{K}_{\alpha,\beta} \triangleq \left\langle \Omega^\alpha, \phi_\beta^{[c_0]} \right\rangle_{\mathbb{H}_N^{[c_0]}},$$

according to the properties of the quasi-orthogonal polynomials  $\phi_\alpha^{[c_0]}$  (3.6) and (3.7), we have

$$\mathcal{K}_{\alpha,\beta} = 0, \text{ when } |\alpha| < |\beta|; \quad \mathcal{K}_{\alpha,\beta} = \left\langle \phi_\alpha^{[c_0]}, \phi_\beta^{[c_0]} \right\rangle_{\mathbb{H}_N^{[c_0]}} = \mathcal{K}_{\beta,\alpha}, \text{ when } |\alpha| = |\beta|.$$

Let us denote the matrix composed of

$$\mathcal{K}_{\alpha,\beta}, \quad \alpha, \beta \in \mathcal{I}_N, |\alpha| = i, |\beta| = j,$$

as  $\mathcal{K}_{i,j}$ , whose dimension is  $(2i + 1) \times (2j + 1)$ . It is not difficult to show that

1.  $\mathcal{K}_{i,j} = 0$ , when  $i < j$ .
2.  $\mathcal{K}_{k,k}$  is symmetric and positive definite.

Then, by the Gram-Schmidt orthogonalization, the calculation of the quasi-orthogonal polynomials can be written as

$$\phi_j^{[c_0]} = \varphi_j - \sum_{k=0}^{j-1} \mathcal{K}_{j,k} \mathcal{K}_{k,k}^{-1} \phi_k^{[c_0]}, \quad j \geq 0. \quad (3.10)$$

Taking the inner product of  $\varphi_i$  and the transpose of (3.10), one can derive the recursion relation of coefficients  $\mathcal{K}_{\alpha,\beta}$ ,

$$\mathcal{K}_{i,j} = \langle \varphi_i, \varphi_j^T \rangle_{\mathbb{H}_N^{[c_0]}} - \sum_{k=0}^{j-1} \mathcal{K}_{i,k} \mathcal{K}_{k,k}^{-1} \mathcal{K}_{j,k}^T. \quad (3.11)$$

Therefore, once  $\mathcal{E}_\alpha$  are calculated,  $\mathcal{K}_{\alpha,\beta}$  is determined by (3.11), and  $\phi_\alpha^{[c_0]}$  is determined by (3.10). We note that all these formulations are explicit. The details of the calculation of  $\mathcal{E}_\alpha$  are presented in Subsection 3.2.

Since the quasi-orthogonal polynomials have been calculated, one can simply determine the coefficients  $f_\alpha$  by the constraints of the known moments. To be precise,  $\langle \hat{I} \rangle_k = \mathbf{E}_k$  implies that

$$\sum_{j=0}^k \mathcal{K}_{k,j} \mathbf{f}_j = \mathbf{E}_k, \quad 0 \leq k \leq N, \quad (3.12)$$

thus the coefficients  $f_\alpha$ ,  $\alpha \in \mathcal{I}_N$  are obtained by

$$\mathbf{f}_k = \mathcal{K}_{k,k}^{-1} \left( \mathbf{E}_k - \sum_{j=0}^{k-1} \mathcal{K}_{k,j} \mathbf{f}_j \right), \quad 0 \leq k \leq N. \quad (3.13)$$

Eventually, the moment closure of the  $MP_N$  model is given as

$$\mathbf{E}_{N+1} = \langle \hat{I} \rangle_{N+1} = \sum_{j=0}^N \kappa_{N+1,j} \mathbf{f}_j. \quad (3.14)$$

Substituting (3.14) into (2.13), a closed moment system is attained. We refer this model as the *3D  $MP_N$  moment system* later on.

**Remark 2.** Notice that  $\mathbf{c}_0$  and the weight function  $\omega^{[\mathbf{c}_0]}$  are determined by  $\mathbf{E}_0$  and  $\mathbf{E}_1$ , therefore

$$\frac{\langle \hat{I} \rangle_{e_d}}{\langle \hat{I} \rangle_0} = \frac{E_{e_d}}{E_0} = \frac{\langle \omega^{[\mathbf{c}_0]} \rangle_{e_d}}{\langle \omega^{[\mathbf{c}_0]} \rangle_0} = \frac{\mathcal{K}_{e_d,0}}{\mathcal{K}_{0,0}}, \quad d = 1, 2, 3.$$

Simple calculation yields

$$f_0 = E_0 / \mathcal{K}_{0,0}, \quad E_{e_d} - \mathcal{K}_{e_d,0} f_0 = 0, \quad d = 1, 2, 3,$$

which tells that

$$f_{e_d} = 0, \quad d = 1, 2, 3. \quad (3.15)$$

It is essential for a reduced model to preserve the Galilean invariance of 3D RTE (2.1). It is often trivial to preserve the reduced model to be invariant under a translation. However, only both with translational invariance and rotational invariance, the reduced model in 3D is Galilean invariant. Unfortunately, the rotational invariance is not usually preserved by the model reduction of 3D RTE automatically. For instance, the extensively used  $S_N$  model, due to the lack of the rotational invariance, leads to the so-called *ray-effect* in numerical simulations, which is regarded as its major flaw [28].

Thanks to the rotational invariance of the weight function (the 3D  $M_1$  model), the rotational invariance of the 3D  $MP_N$  model is trivial to be verified. We denote the orthogonal coordinate system as  $(\mathbf{e}_x, \mathbf{e}_y, \mathbf{e}_z)$ , and the coordinate of an element  $\mathbf{p}$  is  $\mathbf{x} = (\mathbf{p} \cdot \mathbf{e}_x, \mathbf{p} \cdot \mathbf{e}_y, \mathbf{p} \cdot \mathbf{e}_z)^T$ . After a given rotation, the orthogonal coordinate system becomes  $(\overline{\mathbf{e}}_x, \overline{\mathbf{e}}_y, \overline{\mathbf{e}}_z)$ , and there is a constant  $3 \times 3$  orthogonal matrix  $\mathbf{G}_1$ , with  $\text{Det}(\mathbf{G}_1) = 1$ , satisfies that  $(\overline{\mathbf{e}}_x, \overline{\mathbf{e}}_y, \overline{\mathbf{e}}_z) = (\mathbf{e}_x, \mathbf{e}_y, \mathbf{e}_z) \mathbf{G}_1^T$ , then the coordinate of the same element  $\mathbf{p}$  is given by  $\overline{\mathbf{x}} = (\mathbf{p} \cdot \overline{\mathbf{e}}_x, \mathbf{p} \cdot \overline{\mathbf{e}}_y, \mathbf{p} \cdot \overline{\mathbf{e}}_z)^T = \mathbf{G}_1 \mathbf{x}$ . Then the moments in the rotated system can be written as a linear combination of the moments in the original system. For any given  $k \in \mathbb{N}$ , there exists a non-singular  $(2k+1) \times (2k+1)$  matrix  $\mathbf{G}_k$ , satisfying that

$$\overline{\boldsymbol{\varphi}}_k = \mathbf{G}_k \boldsymbol{\varphi}_k, \quad k \geq 0,$$

where  $\boldsymbol{\varphi}_k$  and  $\overline{\boldsymbol{\varphi}}_k$  are the vectors of the  $k$ -th moment of the weight function, defined in Subsection 3.1, in the original system and the rotated system, respectively. Furthermore, in the rotated system, the moments are denoted as  $\overline{\mathbf{E}}_k$ ,  $0 \leq k \leq N$ . One can directly verify that

$$\overline{\mathbf{E}}_k = \mathbf{G}_k \mathbf{E}_k, \quad 0 \leq k \leq N.$$

Let us give a lemma at first.

**Lemma 2.**

$$\mathcal{D}_{\mathbf{G}_1 \mathbf{x}}(\mathbf{G}_{k+1} \mathbf{E}_{k+1}) = \mathbf{G}_k \mathcal{D}_{\mathbf{x}}(\mathbf{E}_{k+1}), \quad k \geq 0,$$

where  $\mathcal{D}_{\mathbf{x}}(\mathbf{E}_{k+1})$  is defined as a  $(2k+1)$ -vector corresponding to  $\mathbf{E}_k$ . More accurately, if the  $\mathcal{N}(\alpha, k)$ -th element of  $\mathbf{E}_k$  is  $E_\alpha$ ,  $|\alpha| = k$ , then the  $\mathcal{N}(\alpha, k)$ -th element of  $\mathcal{D}_{\mathbf{x}}(\mathbf{E}_{k+1})$  is  $\sum_{d=1}^3 \frac{\partial E_{\alpha+e_d}}{\partial x_d}$ .

*Proof.* Noticing  $\overline{\boldsymbol{\varphi}}_k = \mathbf{G}_k \boldsymbol{\varphi}_k$ , and the  $\mathcal{N}(\alpha, k)$ -th element of  $\boldsymbol{\varphi}_k$  is  $\Omega^\alpha$ , we have

$$(\mathbf{G}_1 \Omega)^\alpha = \sum_{|\beta|=k, \beta \in \mathcal{I}} \mathbf{G}_{k, \mathcal{N}(\alpha, k), \mathcal{N}(\beta, k)} \Omega^\beta, \quad |\alpha| = k, \alpha \in \mathcal{I}, \quad (3.16)$$

and  $\overline{\mathbf{E}}_k = \mathbf{G}_k \mathbf{E}_k$  can be rewritten as

$$\overline{E}_\alpha = \sum_{|\beta|=k, \beta \in \mathcal{I}} \mathbf{G}_{k, \mathcal{N}(\alpha, k), \mathcal{N}(\beta, k)} E_\beta, \quad |\alpha| = k, \alpha \in \mathcal{I}. \quad (3.17)$$



Moreover, multiplying  $(\mathbf{G}_1 \boldsymbol{\Omega})^{e_d}$  on (3.16), one has

$$\begin{aligned} (\mathbf{G}_1 \boldsymbol{\Omega})^{\alpha+e_d} &= \sum_{|\beta|=k, \beta \in \mathcal{I}} \mathbf{G}_{k, \mathcal{N}(\alpha, k), \mathcal{N}(\beta, k)} \boldsymbol{\Omega}^\beta (\mathbf{G}_1 \boldsymbol{\Omega})^{e_d} \\ &= \sum_{l=1}^3 \sum_{|\beta|=k, \beta \in \mathcal{I}} \mathbf{G}_{k, \mathcal{N}(\alpha, k), \mathcal{N}(\beta, k)} \mathbf{G}_{1, d, l} \boldsymbol{\Omega}^{\beta+e_l}, \quad |\alpha| = k, \alpha \in \mathcal{I}, \end{aligned}$$

which is equivalent to

$$\overline{E_{\alpha+e_d}} = \sum_{l=1}^3 \sum_{|\beta|=k, \beta \in \mathcal{I}} \mathbf{G}_{k, \mathcal{N}(\alpha, k), \mathcal{N}(\beta, k)} \mathbf{G}_{1, d, l} E_{\beta+e_l}, \quad |\alpha| = k, \alpha \in \mathcal{I}, d = 1, 2, 3.$$

Noticing  $\overline{x_d} = \sum_{s=1}^3 \mathbf{G}_{1, d, s} x_s$  and  $\mathbf{G}_1$  is a orthogonal matrix, one has  $x_s = \sum_{d=1}^3 \mathbf{G}_{1, s, d}^T \overline{x_d} = \sum_{d=1}^3 \mathbf{G}_{1, d, s} \overline{x_d}$ , and

$$\begin{aligned} \sum_{d=1}^3 \frac{\partial \overline{E_{\alpha+e_d}}}{\partial \overline{x_d}} &= \sum_{d=1}^3 \sum_{s=1}^3 \frac{\partial \left( \sum_{l=1}^3 \sum_{|\beta|=k, \beta \in \mathcal{I}} \mathbf{G}_{k, \mathcal{N}(\alpha, k), \mathcal{N}(\beta, k)} \mathbf{G}_{1, d, l} E_{\beta+e_l} \right)}{\partial x_s} \frac{\partial x_s}{\partial \overline{x_d}} \\ &= \sum_{|\beta|=k, \beta \in \mathcal{I}} \sum_{d, l, s=1}^3 \mathbf{G}_{k, \mathcal{N}(\alpha, k), \mathcal{N}(\beta, k)} \mathbf{G}_{1, d, l} \frac{\partial E_{\beta+e_l}}{\partial x_s} \mathbf{G}_{1, d, s} \\ &= \sum_{l=1}^3 \sum_{|\beta|=k, \beta \in \mathcal{I}} \mathbf{G}_{k, \mathcal{N}(\alpha, k), \mathcal{N}(\beta, k)} \frac{\partial E_{\beta+e_l}}{\partial x_l}. \end{aligned} \tag{3.18}$$

Compare (3.18) with (3.17), one can yield

$$\mathcal{D}_{\mathbf{G}_1 \mathbf{x}}(\mathbf{G}_{k+1} \mathbf{E}_{k+1}) = \mathbf{G}_k \mathcal{D}_{\mathbf{x}}(\mathbf{E}_{k+1}), \quad k \geq 0.$$

□

For  $0 \leq k \leq N-1$ , the 3D  $MP_N$  system for the  $k$ -th order moment can be written as

$$\frac{1}{c} \frac{\partial \mathbf{E}_k}{\partial t} + \mathcal{D}_{\mathbf{x}}(\mathbf{E}_{k+1}) = \mathbf{S}_k, \tag{3.19}$$

and

$$\frac{1}{c} \frac{\partial \overline{\mathbf{E}}_k}{\partial t} + \mathcal{D}_{\overline{\mathbf{x}}}(\overline{\mathbf{E}}_{k+1}) = \overline{\mathbf{S}}_k, \tag{3.20}$$

in the original coordinate system and rotated coordinate system, respectively, where  $\mathbf{S}_k$  and  $\overline{\mathbf{S}}_k$  are the vectors of  $S_\alpha$ ,  $|\alpha| = k$  in the original system and rotated system. According to Lemma 2 and noticing  $\overline{\mathbf{E}}_k = \mathbf{G}_k \mathbf{E}_k$ ,  $\overline{\mathbf{x}} = \mathbf{G}_1 \mathbf{x}$ , we have that (3.20) is equivalent to

$$\frac{1}{c} \mathbf{G}_k \frac{\partial \mathbf{E}_k}{\partial t} + \mathbf{G}_k \mathcal{D}_{\overline{\mathbf{x}}}(\overline{\mathbf{E}}_{k+1}) = \mathbf{G}_k \overline{\mathbf{S}}_k,$$

thus we obtain the rotational invariance for  $0 \leq k \leq N-1$ . Meanwhile, the governing equations of the  $N$ -th moment in the original system and rotated system are

$$\frac{1}{c} \frac{\partial \mathbf{E}_N}{\partial t} + \mathcal{D}_{\mathbf{x}}(\mathbf{E}_{N+1}) = \mathbf{S}_N, \tag{3.21}$$

and

$$\frac{1}{c} \frac{\partial \overline{\mathbf{E}}_N}{\partial t} + \mathcal{D}_{\overline{\mathbf{x}}}(\overline{\mathbf{E}}_{N+1}(\overline{\mathbf{E}}_k, 0 \leq k \leq N)) = \overline{\mathbf{S}}_N. \tag{3.22}$$

Therefore in order to obtain the rotational invariance, one only needs to show that based on the rotated known moments  $\overline{\mathbf{E}}_k$ ,  $0 \leq k \leq N$ , the moment closure of the 3D  $MP_N$  model would give the rotated  $(N+1)$ -th moments  $\overline{\mathbf{E}}_{N+1}$ , i.e.

$$\mathbf{E}_{N+1}(\overline{\mathbf{E}}_k, 0 \leq k \leq N) = \overline{\mathbf{E}_{N+1}(\mathbf{E}_k, 0 \leq k \leq N)} = \mathbf{G}_{N+1} \mathbf{E}_{N+1}.$$

Apart from the moments  $\overline{\boldsymbol{\varphi}}_k$  and  $\overline{\mathbf{E}}_k$ , in the following discussion, we denote the variables with an overline  $\overline{\ast}$  as the variables in the rotated coordinate system, such as  $\overline{\mathbf{c}}_0$ ,  $\overline{\omega^{[c_0]}}$ ,  $\overline{\mathbf{f}}_k$ , and  $\overline{\mathcal{K}_{i,j}}$ . Then we arrive the following theorem:

**Theorem 3.** *The 3D MP<sub>N</sub> model is rotational invariant.*

*Proof.* First, we consider the rotational invariance of the weight function. According to the expression of  $\mathbf{c}_0$  (3.2), we have for the rotated system,  $\overline{\mathbf{c}}_0 = \mathbf{G}_1 \mathbf{c}_0$ , thus the weight function is

$$\overline{\omega^{[\mathbf{c}_0]}}(\boldsymbol{\Omega}) = \omega^{[\mathbf{c}_0]}(\boldsymbol{\Omega}) = \frac{1}{(1 + \overline{\mathbf{c}}_0 \cdot \boldsymbol{\Omega})^4}.$$

Notice that  $\overline{\mathbf{c}}_0 \cdot \mathbf{G}_1 \boldsymbol{\Omega} = \mathbf{c}_0^T \mathbf{G}_1^T \mathbf{G}_1 \boldsymbol{\Omega} = \mathbf{c}_0 \cdot \boldsymbol{\Omega}$ , we have

$$\overline{\omega^{[\mathbf{c}_0]}}(\mathbf{G}_1 \boldsymbol{\Omega}) = \omega^{[\mathbf{c}_0]}(\boldsymbol{\Omega}). \quad (3.23)$$

Moreover, on the moments of the weight function, we have

$$\int_{\mathbb{S}^2} \boldsymbol{\varphi}_i \boldsymbol{\varphi}_j^T \overline{\omega^{[\mathbf{c}_0]}(\boldsymbol{\Omega})} d\boldsymbol{\Omega} = \int_{\mathbb{S}^2} \mathbf{G}_i \boldsymbol{\varphi}_i \boldsymbol{\varphi}_j^T \mathbf{G}_j^T \omega^{[\mathbf{c}_0]}(\boldsymbol{\Omega}) d\boldsymbol{\Omega} = \mathbf{G}_i \langle \boldsymbol{\varphi}_i, \boldsymbol{\varphi}_j^T \rangle_{\mathbb{H}_N^{[\mathbf{c}_0]}} \mathbf{G}_j^T, \quad (3.24)$$

where the first equality is according to (3.23) and using a variable substitution (replace  $\boldsymbol{\Omega}$  by  $\mathbf{G}_1 \boldsymbol{\Omega}$ ). Therefore, according to (3.11) and (3.24), using mathematical methods of induction, we have the coefficient matrix in the new coordinate system  $\overline{\mathcal{K}}_{i,j}$  satisfies that

$$\overline{\mathcal{K}}_{i,j} = \mathbf{G}_i \mathcal{K}_{i,j} \mathbf{G}_j^T.$$

Analogously, by (3.13), we have  $\overline{\mathbf{f}}_k = \mathbf{G}_k \mathbf{f}_k$ . Then by (3.14), the moment closure is  $\mathbf{G}_{N+1} \mathbf{E}_{N+1} = \overline{\mathbf{E}_{N+1}}$ , which ends the proof.  $\square$

### 3.2 Implementation details

**Calculation of  $\mathcal{E}_\alpha$**  In Subsection 3.1, the calculation of the Gram-Schmidt orthogonalization requires a practical method to obtain  $\mathcal{E}_\alpha$ . However, the calculation of  $\mathcal{E}_\alpha$  is not trivial. In this subsection, we present the way to calculate  $\mathcal{E}_\alpha$ .

Let  $\mathbf{c} = \frac{\mathbf{c}_0}{\|\mathbf{c}_0\|}$ , and  $\mathbf{a}, \mathbf{b}, \mathbf{c}$  is a unit orthogonal basis of  $\mathbb{R}^3$ , then we can decompose  $\boldsymbol{\Omega}$  under this basis, i.e.

$$\boldsymbol{\Omega} \cdot \mathbf{a} = \sin \theta \cos \varphi, \quad \boldsymbol{\Omega} \cdot \mathbf{b} = \sin \theta \sin \varphi, \quad \boldsymbol{\Omega} \cdot \mathbf{c} = \cos \theta, \quad 0 \leq \theta < \pi, \quad 0 \leq \varphi < 2\pi,$$

then we have  $\boldsymbol{\Omega} = (\boldsymbol{\Omega} \cdot \mathbf{a})\mathbf{a} + (\boldsymbol{\Omega} \cdot \mathbf{b})\mathbf{b} + (\boldsymbol{\Omega} \cdot \mathbf{c})\mathbf{c}$ , and

$$\mathcal{E}_\alpha = \int_{\mathbb{S}^2} \boldsymbol{\Omega}^\alpha \omega^{[\mathbf{c}_0]}(\boldsymbol{\Omega}) d\boldsymbol{\Omega} = \int_0^{2\pi} \int_0^\pi \frac{\Omega_1^{\alpha_1} \Omega_2^{\alpha_2} \Omega_3^{\alpha_3}}{(1 + \|\mathbf{c}_0\| \cos \theta)^4} \sin \theta d\theta d\varphi.$$

Notice that

$$\begin{aligned} \Omega_1 &= a_1 \sin \theta \cos \varphi + b_1 \sin \theta \sin \varphi + c_1 \cos \theta, \\ \Omega_2 &= a_2 \sin \theta \cos \varphi + b_2 \sin \theta \sin \varphi + c_2 \cos \theta, \\ \Omega_3 &= a_3 \sin \theta \cos \varphi + b_3 \sin \theta \sin \varphi + c_3 \cos \theta, \end{aligned}$$

we have

$$\begin{aligned} \Omega_k^{\alpha_k} &= (a_k \sin \theta \cos \varphi + b_k \sin \theta \sin \varphi + c_k \cos \theta)^{\alpha_k} \\ &= \sum_{n_k \leq m_k \leq \alpha_k} \frac{\alpha_k!}{(m_k - n_k)! n_k! (\alpha_k - m_k)!} (a_k \sin \theta \cos \varphi)^{m_k - n_k} (b_k \sin \theta \sin \varphi)^{n_k} (c_k \cos \theta)^{\alpha_k - m_k} \\ &= \sum_{n_k \leq m_k \leq \alpha_k} \frac{\alpha_k!}{(m_k - n_k)! n_k! (\alpha_k - m_k)!} a_k^{m_k - n_k} b_k^{n_k} c_k^{\alpha_k - m_k} \sin^{m_k} \theta \cos^{\alpha_k - m_k} \theta \cos^{m_k - n_k} \varphi \sin^{n_k} \varphi. \end{aligned}$$

Collecting the terms, we have

$$\boldsymbol{\Omega}^\alpha = \prod_{k=1}^3 \Omega_k^{\alpha_k} = \sum_{n \leq m \leq |\alpha|} C_{m,n}^{\alpha_1, \alpha_2, \alpha_3} \sin^m \theta \cos^{|\alpha| - m} \theta \sin^n \varphi \cos^{m - n} \varphi,$$

where  $C_{m,n}^{\alpha_1, \alpha_2, \alpha_3}$  are coefficients. Precisely, denote  $C_{m,n}^\alpha = C_{m,n}^{\alpha_1, \alpha_2, \alpha_3}$ , then one can obtain the recursion relationship of  $C_{m,n}^\alpha$ , formulated as

$$C_{m,n}^\alpha = c_k C_{m,n}^{\alpha - e_k} + a_k C_{m-1,n}^{\alpha - e_k} + b_k C_{m-1,n-1}^{\alpha - e_k}, \quad k = 1, 2, 3,$$

Furthermore, we can obtain  $\mathcal{E}_\alpha$  by

$$\mathcal{E}_\alpha = \sum_{n \leq m \leq |\alpha|} C_{m,n}^{\alpha_1, \alpha_2, \alpha_3} \int_0^\pi \frac{\sin^{m+1} \theta \cos^{|\alpha|-m} \theta}{(1 + c_0 \cos \theta)^4} d\theta \int_0^{2\pi} \sin^n \varphi \cos^{m-n} \varphi d\varphi.$$

Direct calculation yields

$$I_{|\alpha|,m} = \int_0^\pi \frac{\sin^{m+1} \theta \cos^{|\alpha|-m} \theta}{(1 + c_0 \cos \theta)^4} d\theta = \int_{-1}^1 \frac{(1 - \mu^2)^{m/2} \mu^{|\alpha|-m}}{(1 + c_0 \mu)^4} d\mu = \sum_{l=0}^{m/2} \binom{m/2}{l} (-1)^l M_{|\alpha|-m+2l},$$

where  $M_s = \int_{-1}^1 \frac{\mu^s}{(1 + c_0 \mu)^4} d\mu$  has already been calculated in the 1D  $MP_N$  model [20]. On the other hand,

$$J_{n,m-n} = \int_0^{2\pi} \sin^n \varphi \cos^{m-n} \varphi d\varphi = \begin{cases} \frac{2\Gamma(\frac{1+m-n}{2}) \Gamma(\frac{1+n}{2})}{\Gamma(\frac{m+2}{2})}, & m, n \text{ are even,} \\ 0, & \text{otherwise.} \end{cases}$$

Moreover, when  $m$  and  $n$  are even,

$$J_{n,m-n} = \frac{2\Gamma(\frac{1+m-n}{2}) \Gamma(\frac{1+n}{2})}{\Gamma(\frac{m+2}{2})} = 2\pi \frac{(m-n-1)!!(n-1)!!}{2^{\frac{m-n}{2}} 2^{\frac{n}{2}} (\frac{m}{2})!} = 2\pi \frac{(m-n-1)!!(n-1)!!}{2^{\frac{m}{2}} (\frac{m}{2})!}.$$

Therefore, we have

$$\mathcal{E}_\alpha = \sum_{n \leq m \leq |\alpha|} C_{m,n}^{\alpha_1, \alpha_2, \alpha_3} I_{|\alpha|,m} J_{n,m-n}.$$

**Remark 3.** The choice of  $\mathbf{a}$ ,  $\mathbf{b}$ , and  $\mathbf{c}$  can be casual. For example, if  $\mathbf{c} = (\sin \theta_0 \cos \varphi_0, \sin \theta_0 \sin \varphi_0, \cos \theta_0)^T$ , then  $\mathbf{a}$ ,  $\mathbf{b}$ , and  $\mathbf{c}$  can be chosen as

$$[\mathbf{a}, \mathbf{b}, \mathbf{c}] = \begin{bmatrix} \sin \varphi_0 & \cos \theta_0 \cos \varphi_0 & \sin \theta_0 \cos \varphi_0 \\ -\cos \varphi_0 & \cos \theta_0 \sin \varphi_0 & \sin \theta_0 \sin \varphi_0 \\ 0 & -\sin \theta_0 & \cos \theta_0 \end{bmatrix}.$$

**Interpolation** In Subsection 3.1, a Gram-Schmidt orthogonalization is adopted to evaluate the moment closure. However, the cost of the orthogonalization is  $O(N^6)$ , which is a difficult issue in the numerical simulations. In [20], thanks to the linear dependence of the moment closure on  $\mathbf{E}_k$ ,  $2 \leq k \leq N$ , an interpolation is applied to reduce the cost. In the 3D  $MP_N$  model, the dependence of the moment closure  $\mathbf{E}_{N+1}$  upon  $\mathbf{E}_k$ ,  $2 \leq k \leq N$  is linear. Precisely, we have

$$\mathbf{E}_{N+1} = \sum_{k=0}^N \mathbf{C}_k(\mathbf{c}_0) \mathbf{E}_k,$$

where  $\mathbf{C}_k(\mathbf{c}_0)$  is a  $(2N+3) \times (2k+1)$  matrix, which depends on  $\mathbf{c}_0$  only. Therefore, a naive idea is to divide the unit sphere  $\mathbb{S}^2$  into several parts, and apply the interpolation. However, in order to get a sufficient accuracy, dividing the unit sphere will cost a lot, thus we need another interpolation method.

Noticing the rotational invariance of the 3D  $MP_N$  model and the  $HMP_N$  model, we can calculate the moment closure  $\overline{\mathbf{E}_{N+1}}$  corresponding to  $\overline{\mathbf{c}_0} = \mathbf{G}_1 \mathbf{c}_0$ , satisfying that  $\overline{\mathbf{c}_0}$  is parallel to  $\mathbf{e}_z$ . The procedure of the evaluation of the moment closure  $\mathbf{E}_{N+1}$  can be written as

1. Calculate  $\mathbf{c}_0$ ,  $\overline{\mathbf{c}_0}$ .
2. Calculate the matrix  $\mathbf{G}_k$ ,  $1 \leq k \leq N+1$ , whose cost is  $O(N^3)$ .
3. Calculate  $\overline{\mathbf{E}_k}$ ,  $0 \leq k \leq N$  by

$$\overline{\mathbf{E}_k} = \mathbf{G}_k \mathbf{E}_k,$$

and the cost is  $O(N^3)$ .

4. Calculate  $\overline{\mathbf{E}_{N+1}}$  by interpolation, the cost is  $O(N^3)$ .
5. Calculate  $\mathbf{E}_{N+1}$  by

$$\mathbf{E}_{N+1} = \mathbf{G}_{N+1}^{-1} \overline{\mathbf{E}_{N+1}},$$

the cost is  $O(N^2)$ .

Therefore, by this interpolation, we reduce the cost of the evolution of the moment closure to  $O(N^3)$ , which broadens the application of the  $MP_N$  model.

## 4 Hyperbolic Regularization

Similar as the 1D  $MP_N$  model, the 3D  $MP_N$  model needs to be regularized to achieve global hyperbolicity. We follow the idea in [19] to propose a novel hyperbolic regularization for the 3D  $MP_N$  model.

At first, we introduce the orthogonal projection to the function space  $\mathbb{H}_N^{[c_0]}$  in (3.3),

$$\mathcal{P}_N : f = \sum_{\alpha \in \mathcal{I}} f_\alpha \phi_\alpha^{[c_0]} \longrightarrow \mathcal{P}_N f = \sum_{\alpha \in \mathcal{I}_N} f_\alpha \phi_\alpha^{[c_0]}. \quad (4.1)$$

Then the 3D  $MP_N$  moment system can be formulated as

$$\frac{1}{c} \mathcal{P}_N \frac{\partial \mathcal{P}_N I}{\partial t} + \sum_{d=1}^3 \mathcal{P}_N \Omega_d \frac{\partial \mathcal{P}_N I}{\partial x_d} = \mathcal{P}_N \mathcal{S}(\mathcal{P}_N I). \quad (4.2)$$

Using the similar method in [19], we introduce a new weight function

$$\tilde{\omega}^{[c_0]}(\mathbf{\Omega}) = \frac{1}{(1 + \mathbf{c}_0 \cdot \mathbf{\Omega})^5}, \quad (4.3)$$

and the relationship between the weight function  $\omega^{[c_0]}$  and the new weight function  $\tilde{\omega}^{[c_0]}$  is

$$\omega^{[c_0]}(\mathbf{\Omega}) = (1 + \mathbf{c}_0 \cdot \mathbf{\Omega}) \tilde{\omega}^{[c_0]}(\mathbf{\Omega}), \quad \nabla_{\mathbf{c}_0} \omega^{[c_0]}(\mathbf{\Omega}) = -4 \mathbf{\Omega} \tilde{\omega}^{[c_0]}(\mathbf{\Omega})$$

Based on the new weight function, we can also define the function space  $\tilde{\mathbb{H}}_N^{[c_0]}$ , the quasi-orthogonal polynomials  $\tilde{\phi}_\alpha^{[c_0]}$ ,  $\alpha \in \mathcal{I}_N$ , the quasi-orthogonal functions  $\tilde{\Phi}_\alpha^{[c_0]}$ , the coefficients  $\tilde{\mathcal{K}}_{\alpha,\beta}$ , and the orthogonal projection  $\tilde{\mathcal{P}}_N$ .

Then, according to the hyperbolic regularization used in [19], the 3D  $HMP_N$  model can be written as

$$\frac{1}{c} \tilde{\mathcal{P}}_N \frac{\partial \mathcal{P}_N I}{\partial t} + \sum_{d=1}^3 \tilde{\mathcal{P}}_N \Omega_d \tilde{\mathcal{P}}_N \frac{\partial \mathcal{P}_N I}{\partial x_d} = \tilde{\mathcal{P}}_N \mathcal{S}(\mathcal{P}_N I). \quad (4.4)$$

Let us show the details of the regularization. In order to calculate the difference between the  $HMP_N$  model (4.4) and the  $MP_N$  model (4.2), here we first introduce a lemma.

**Lemma 4.**

$$\Phi_\alpha^{[c_0]} \in \mathbb{H}_N^{[c_0]} \subset \tilde{\mathbb{H}}_{N+1}^{[c_0]}, \quad \frac{\partial \Phi_\alpha^{[c_0]}}{\partial c_{0,d}} \in \tilde{\mathbb{H}}_{N+1}^{[c_0]}, \quad |\alpha| \leq N, \quad d = 1, 2, 3.$$

*Proof.* In this proof, we only consider the situation when  $|\alpha| = N$ . We have

$$\begin{aligned} \Phi_\alpha^{[c_0]} &= \omega^{[c_0]} \phi_\alpha^{[c_0]} = \tilde{\omega}^{[c_0]} \phi_\alpha^{[c_0]} (1 + \mathbf{c}_0 \cdot \mathbf{\Omega}), \\ \frac{\partial \Phi_\alpha^{[c_0]}}{\partial c_{0,d}} &= \frac{\partial \omega^{[c_0]}}{\partial c_{0,d}} \phi_\alpha^{[c_0]} + \omega^{[c_0]} \frac{\partial \phi_\alpha^{[c_0]}}{\partial c_{0,d}} = -4 \Omega_d \tilde{\omega}^{[c_0]} \phi_\alpha^{[c_0]} + (1 + \mathbf{c}_0 \cdot \mathbf{\Omega}) \tilde{\omega}^{[c_0]} \frac{\partial \phi_\alpha^{[c_0]}}{\partial c_{0,d}}. \end{aligned}$$

We have  $\tilde{\omega}^{[c_0]} \phi_\alpha^{[c_0]} \in \tilde{\mathbb{H}}_N^{[c_0]}$  and  $(1 + \mathbf{c}_0 \cdot \mathbf{\Omega}) \tilde{\omega}^{[c_0]} \frac{\partial \phi_\alpha^{[c_0]}}{\partial c_{0,d}} \in \tilde{\mathbb{H}}_N^{[c_0]}$ , thus

$$\Phi_\alpha^{[c_0]} - \tilde{\mathcal{P}}_N \Phi_\alpha^{[c_0]} = (I - \tilde{\mathcal{P}}_N)(\tilde{\omega}^{[c_0]} \mathbf{c}_0 \cdot \mathbf{\Omega} \phi_\alpha^{[c_0]}) = \sum_{d=1}^3 c_{0,d} \tilde{\Phi}_{\alpha+e_d}^{[c_0]},$$

$$\frac{\partial \Phi_\alpha^{[c_0]}}{\partial c_{0,d}} - \tilde{\mathcal{P}}_N \frac{\partial \Phi_\alpha^{[c_0]}}{\partial c_{0,d}} = -4 \tilde{\Phi}_{\alpha+e_d}^{[c_0]}.$$

□

According to the proof of Lemma 4, we have

**Corollary 5.**

$$\Phi_{\alpha}^{[c_0]} - \tilde{\mathcal{P}}_N \Phi_{\alpha}^{[c_0]} = \begin{cases} 0, & |\alpha| < N, \\ \sum_{d=1}^3 c_{0,d} \tilde{\Phi}_{\alpha+e_d}^{[c_0]}, & |\alpha| = N. \end{cases},$$

$$\frac{\partial \Phi_{\alpha}^{[c_0]}}{\partial c_{0,d}} - \tilde{\mathcal{P}}_N \frac{\partial \Phi_{\alpha}^{[c_0]}}{\partial c_{0,d}} = \begin{cases} 0, & |\alpha| < N, \\ -4 \tilde{\Phi}_{\alpha+e_d}^{[c_0]}, & |\alpha| = N. \end{cases},$$

Substituting the terms in Corollary 5 to (4.4), the difference between the  $HMP_N$  system and the  $MP_N$  system is

$$\begin{aligned} & \sum_{d=1}^3 \tilde{\mathcal{P}}_N \Omega_d \left( \tilde{\mathcal{P}}_N \frac{\partial \mathcal{P}_N I}{\partial x_d} - \frac{\partial \mathcal{P}_N I}{\partial x_d} \right) \\ &= \sum_{d=1}^3 \tilde{\mathcal{P}}_N \Omega_d \left( \tilde{\mathcal{P}}_N \frac{\partial \left( \sum_{\alpha \in \mathcal{I}_N} \delta_{|\alpha|,N} f_{\alpha} \Phi_{\alpha}^{[c_0]} \right)}{\partial x_d} - \frac{\partial \left( \sum_{\alpha \in \mathcal{I}_N} \delta_{|\alpha|,N} f_{\alpha} \Phi_{\alpha}^{[c_0]} \right)}{\partial x_d} \right) \\ &= \sum_{d=1}^3 \tilde{\mathcal{P}}_N \Omega_d \left( \sum_{\alpha \in \mathcal{I}_N} \delta_{|\alpha|,N} \left( \sum_{l=1}^3 4 f_{\alpha} \tilde{\Phi}_{\alpha+e_l}^{[c_0]} \frac{\partial c_{0,l}}{\partial x_d} - \frac{\partial f_{\alpha}}{\partial x_d} \sum_{l=1}^3 c_{0,l} \tilde{\Phi}_{\alpha+e_l}^{[c_0]} \right) \right), \end{aligned} \quad (4.5)$$

where  $\delta_{i,j}$  is the Kronecker delta. Then one can consider the inner product of (4.5) with  $\Omega^{\alpha}$  to carry out the  $HMP_N$  system, written as

$$\frac{1}{c} \frac{\partial E_{\alpha}}{\partial t} + \sum_{d=1}^3 \left( \frac{\partial E_{\alpha+e_d}}{\partial x_d} - R_{\alpha,d} \right) = S_{\alpha}, \quad (4.6)$$

where  $S_{\alpha} \triangleq \langle \mathcal{S}(\mathcal{P}_N I) \rangle_{\alpha}$  is the  $\alpha$ -th order moment of the right hand side  $\mathcal{S}(\mathcal{P}_N I)$ , and  $R_{\alpha,d}$ , according to (4.5), is

$$R_{\alpha,d} = \begin{cases} 0, & |\alpha| < N, \\ \sum_{\beta \in \mathcal{I}_N, |\beta|=N} \sum_{l=1}^3 \left( \frac{\partial f_{\beta}}{\partial x_d} c_{0,l} - 4 f_{\beta} \frac{\partial c_{0,l}}{\partial x_d} \right) \tilde{\mathcal{K}}_{\alpha+e_d, \beta+e_l}, & |\alpha| = N. \end{cases} \quad (4.7)$$

**Remark 4.** If  $\alpha + e_d \notin \mathcal{I}$ , i.e.  $\alpha_3 = 1$  and  $d = 3$ , then  $\tilde{\mathcal{K}}_{\alpha+e_d, \beta+e_l}$  can be calculated by

$$\tilde{\mathcal{K}}_{\alpha+e_3, \beta+e_l} = \tilde{\mathcal{K}}_{\alpha-e_3, \beta+e_l} - \tilde{\mathcal{K}}_{\alpha-e_3+2e_1, \beta+e_l} - \tilde{\mathcal{K}}_{\alpha-e_3+2e_2, \beta+e_l}.$$

Analogously, for  $\beta + e_l \notin \mathcal{I}$ ,  $\tilde{\mathcal{K}}_{\alpha+e_d, \beta+e_l}$  can also be calculated.

Therefore, one can conclude that

**Property 6.** The regularization does not change the moment equations for  $E_{\alpha}$ ,  $\alpha \in \mathcal{I}_{N-1}$ .

On the other hand, notice that if  $N = 1$ , according to (4.7) and (3.15), we have that the  $HMP_N$  model is exact the same as the  $MP_N$  model. Thus, as the  $HMP_N$  model in slab geometry [19], we have the following property,

**Property 7.** The hyperbolic regularization in 3D case does not change the  $M_1$  model, in other words, the  $HMP_N$  model is the same as the  $M_1$  model when  $N = 1$ .

In Section 3, the rotational invariance of the 3D  $MP_N$  model has been proved and in this section we investigate the rotational invariance of the 3D  $HMP_N$  model. According to Theorem 3, the remaining part is  $R_{\alpha,d}$  in (4.7), a simple conclusion is given as

**Theorem 8.** The 3D  $HMP_N$  model is rotational invariant.

*Proof.* According to (3.17), one only needs to prove that

$$\sum_{d=1}^3 \overline{R_{\alpha,d}} = \sum_{d=1}^3 \sum_{|\beta|=N, \beta \in \mathcal{I}} \mathbf{G}_{N, \mathcal{N}(\alpha, N), (\beta, N)} R_{\beta,d}, \quad |\alpha| = N, \alpha \in \mathcal{I}. \quad (4.8)$$

According to (4.7), we have

$$\sum_{d=1}^3 \overline{R_{\alpha,d}} = \sum_{d=1}^3 \sum_{|\gamma|=N, \gamma \in \mathcal{I}} \sum_{l=1}^3 \left( \frac{\partial \overline{f_\gamma}}{\partial \overline{x_d}} \overline{c_{0,l}} - 4 \overline{f_\gamma} \frac{\partial \overline{c_{0,l}}}{\partial \overline{x_d}} \right) \overline{\tilde{\mathcal{K}}_{\alpha+e_d, \gamma+e_l}}, \quad |\alpha| = N. \quad (4.9)$$

Noticing that

$$\begin{aligned} \overline{f_\gamma} &= \sum_{|\gamma'|=N, \gamma' \in \mathcal{I}} \mathbf{G}_{N, \mathcal{N}(\gamma, N), \mathcal{N}(\gamma', N)} f_{\gamma'}, \quad \overline{x_d} = \sum_{d'=1}^3 \mathbf{G}_{1, d, d'} x'_{d'}, \quad \overline{c_{0,l}} = \sum_{l'=1}^3 \mathbf{G}_{1, l, l'} c_{0, l'}, \\ \overline{\tilde{\mathcal{K}}_{\alpha+e_d, \gamma+e_l}} &= \sum_{d'', l''=1}^3 \sum_{|\alpha''|=N, \alpha'' \in \mathcal{I}} \sum_{|\gamma''|=N, \gamma'' \in \mathcal{I}} \mathbf{G}_{1, d, d''} \mathbf{G}_{N, \mathcal{N}(\alpha, N), \mathcal{N}(\alpha'', N)} \tilde{\mathcal{K}}_{\alpha''+e_{d''}, \gamma''+e_{l''}} \mathbf{G}_{N, \mathcal{N}(\gamma'', N), \mathcal{N}(\gamma, N)}^T \mathbf{G}_{1, l'', l}^T, \end{aligned}$$

direct calculations yield that (4.9) can be simplified as

$$\sum_{d=1}^3 \overline{R_{\alpha,d}} = \sum_{d=1}^3 \sum_{|\alpha''|=N, \alpha'' \in \mathcal{I}} \mathbf{G}_{N, \mathcal{N}(\alpha, N), \mathcal{N}(\alpha'', N)} R_{\alpha'', d},$$

which is equivalent to (4.8).  $\square$

According to the calculations before, the ansatz  $\hat{I}$  can be determined by the moments  $E_\alpha$ ,  $\alpha \in \mathcal{I}_N$ . According to (3.4), meanwhile, the ansatz can be also determined by  $c_{0,1}, c_{0,2}, c_{0,3}, f_\alpha$ ,  $\alpha \in \mathcal{I}_N$ . Noticing that  $f_{e_1} = f_{e_2} = f_{e_3} = 0$ , we can use a vector  $\mathbf{w} \in \mathbb{R}^{(N+1)^2}$ , which is defined as

$$\mathbf{w} = (f_0, c_{0,1}, c_{0,2}, c_{0,3}, f_\alpha, \alpha \in \mathcal{I}_N, |\alpha| \geq 2)^T, \quad (4.10)$$

to describe the ansatz. Therefore, we can rewrite the  $MP_N$  system (2.13) and the  $HMP_N$  system (4.6) by using the variables  $\mathbf{w}$  instead of  $E_\alpha$ .

Notice that  $\tilde{\mathcal{P}}_N \frac{\partial \mathcal{P}_N I}{\partial s}$ ,  $s = t, x_1, x_2, x_3$ , can be linearly expressed by  $\tilde{\Phi}_\alpha^{[c_0]}$ ,  $\alpha \in \mathcal{I}_N$ , thus there exist a  $(N+1)^2 \times (N+1)^2$  matrix  $\mathbf{D}$ , satisfies that

$$\tilde{\mathcal{P}}_N \frac{\partial \mathcal{P}_N I}{\partial s} = (\tilde{\Phi}^{[c_0]})^T \mathbf{D} \frac{\partial \mathbf{w}}{\partial s}, \quad s = t, x_1, x_2, x_3, \quad (4.11)$$

where  $\tilde{\Phi}^{[c_0]}$  is a vector of all quasi-orthogonal functions  $\tilde{\Phi}_\alpha^{[c_0]}$  for  $\alpha \in \mathcal{I}_N$ , whose dimension is  $(N+1)^2$ . Therefore, the  $HMP_N$  system (4.4) can be rewritten as

$$\frac{1}{c} (\tilde{\Phi}^{[c_0]})^T \mathbf{D} \frac{\partial \mathbf{w}}{\partial t} + \sum_{d=1}^3 \tilde{\mathcal{P}}_N \Omega_d (\tilde{\Phi}^{[c_0]})^T \mathbf{D} \frac{\partial \mathbf{w}}{\partial x_d} = S. \quad (4.12)$$

Taking the inner product of (4.12) with  $\tilde{\Phi}^{[c_0]}$ , one can obtain the matrix form of the  $HMP_N$  system, written as

$$\frac{1}{c} \mathbf{\Lambda} \mathbf{D} \frac{\partial \mathbf{w}}{\partial t} + \sum_{d=1}^3 \mathbf{M}_d \mathbf{D} \frac{\partial \mathbf{w}}{\partial x_d} = \tilde{S}, \quad (4.13)$$

where  $\mathbf{\Lambda}_{\alpha, \beta} = \langle \tilde{\Phi}_\alpha^{[c_0]}, \tilde{\Phi}_\beta^{[c_0]} \rangle_{\mathbb{H}_N^{[c_0]}}$  is symmetric positive definite, and  $\mathbf{M}_{d, \alpha, \beta} = \langle \tilde{\Phi}_\alpha^{[c_0]}, \Omega_d \tilde{\Phi}_\beta^{[c_0]} \rangle_{\mathbb{H}_N^{[c_0]}}$  are symmetric, for  $d = 1, 2, 3$ , and  $\tilde{S}_\alpha = \int_{\mathbb{S}^2} S \tilde{\Phi}_\alpha^{[c_0]} d\Omega$ .

**Theorem 9.** *The 3D  $HMP_N$  model is globally hyperbolic. Precisely,  $\forall \mathbf{n} \in \mathbb{S}^2$ ,  $\mathbf{A} \triangleq c \sum_{d=1}^3 (\mathbf{\Lambda} \mathbf{D})^{-1} (n_d \mathbf{M}_d \mathbf{D})$  is real diagonalizable. Moreover, the eigenvalue of  $\mathbf{A}$  is not greater than the speed of light.*

*Proof.* Notice that, for  $\forall \mathbf{n} \in \mathbb{S}^2$ ,

$$\mathbf{A} = c \sum_{d=1}^3 n_d \mathbf{D}^{-1} \mathbf{\Lambda}^{-1} \mathbf{M}_d \mathbf{D} = \mathbf{D}^{-1} \mathbf{\Lambda}^{-1} \mathbf{M} \mathbf{D},$$

where  $\mathbf{A}$  is symmetric positive definite, and  $\mathbf{M}_{\alpha,\beta} = \left\langle \tilde{\Phi}_\alpha^{[c_0]}, \sum_{d=1}^3 n_d \Omega_d \tilde{\Phi}_\beta^{[c_0]} \right\rangle_{\tilde{\mathbb{H}}_N^{[c_0]}}$  is symmetric, we have that  $\mathbf{A}$  is diagonalisable with real eigenvalues, thus the  $HMP_N$  system is globally hyperbolic.

Moreover, denote  $\lambda$  as the eigenvalue of  $\mathbf{A}$ , then  $\lambda$  is the eigenvalue of  $c\mathbf{A}^{-1}\mathbf{M}$ , and suppose  $\boldsymbol{\xi} \in \mathbb{R}^{(N+1)^2}$  is the corresponding eigenvector, i.e.  $\mathbf{M}\boldsymbol{\xi} = \lambda\mathbf{A}\boldsymbol{\xi}$ . Precisely, denote  $\mathcal{F} = \boldsymbol{\xi}^T \boldsymbol{\Phi}^{[c_0]} \in \tilde{\mathbb{H}}_N^{[c_0]}$ , we have

$$\left\langle \tilde{\Phi}_\alpha^{[c_0]}, \left( c \sum_{d=1}^3 n_d \Omega_d - \lambda \right) \mathcal{F} \right\rangle_{\tilde{\mathbb{H}}_N^{[c_0]}} = 0, \quad \forall \alpha \in \mathcal{I}_N. \quad (4.14)$$

Notice  $\mathcal{F} \in \tilde{\mathbb{H}}_N^{[c_0]}$ , thus (4.14) implies

$$\left\langle \mathcal{F}, \left( c \sum_{d=1}^3 n_d \Omega_d - \lambda \right) \mathcal{F} \right\rangle_{\tilde{\mathbb{H}}_N^{[c_0]}} = 0.$$

Therefore,

$$\lambda = \frac{c \langle \mathcal{F}, (\mathbf{n} \cdot \boldsymbol{\Omega}) \mathcal{F} \rangle_{\tilde{\mathbb{H}}_N^{[c_0]}}}{\langle \mathcal{F}, \mathcal{F} \rangle_{\tilde{\mathbb{H}}_N^{[c_0]}}}.$$

Notice  $|\mathbf{n} \cdot \boldsymbol{\Omega}| \leq 1$ , we have

$$|\lambda| \leq c.$$

□

At the end of this section, we give a summary of the properties of the 3D  $HMP_N$  model.

- The 3D  $HMP_N$  model is rotational invariant.
- The 3D  $HMP_N$  model is globally hyperbolic.
- All the characteristic speeds of the 3D  $HMP_N$  model are not greater than the speed of light.
- The hyperbolic regularization adopted in the 3D  $HMP_N$  model does not change the governing equations of  $E_\alpha$  for  $|\alpha| \leq N-1$  in the 3D  $MP_N$  model.
- The hyperbolic regularization vanishes when  $N=1$ , i.e. the 3D  $HMP_N$  model is exactly the same as the 3D  $MP_N$  model and the 3D  $M_1$  model.

## 5 Numerical Validation

In this section, we try to validate the 3D  $HMP_N$  model by numerical experiments. For this purpose, we first give a preliminary numerical scheme for the regularized reduced model (5.1), and then perform numerical simulations on some typical examples to demonstrate its validity. Due to practical difficulties in a 3D computation and noticing that our aim is to validate the new model, we currently only perform our numerical simulations on 2D domains. Actually, 2D numerical results are enough to demonstrate the major features of our model.

### 5.1 Numerical scheme

We first collect the equations in the regularized reduced model (4.6) in a matrix formation as

$$\frac{1}{c} \frac{\partial \mathbf{U}}{\partial t} + \sum_{d=1}^2 \left[ \frac{\partial \mathbf{F}_d(\mathbf{U})}{\partial x_d} + \mathbf{R}_d(\mathbf{U}) \frac{\partial \mathbf{U}}{\partial x_d} \right] = \mathbf{S}, \quad (5.1)$$

where  $\mathbf{U}$ ,  $\mathbf{F}(\mathbf{U})$ ,  $\mathbf{R}_d \frac{\partial \mathbf{U}}{\partial x_d}$  and  $\mathbf{S}$  are vectors in  $\mathbb{R}^{(N+1)^2}$ , whose  $\alpha$ -th element are  $U_\alpha = E_\alpha$ ,  $F_{d,\alpha} = E_{\alpha+e_d}$ ,

$\left( \mathbf{R}_d \frac{\partial \mathbf{U}}{\partial x_d} \right)_\alpha = R_{\alpha,d}$ , and  $\mathbf{S}_\alpha = S_\alpha$ , respectively.

Denote the computational domain by  $[x_l, x_r] \times [y_l, y_r]$ , where we can make a finite volume discretization conveniently. The domain is partitioned uniformly into  $N_x \times N_y$  cells. The  $(i, j)$ -th mesh cell is

$[x_{i-1/2}, x_{i+1/2}] \times [y_{j-1/2}, y_{j+1/2}]$ ,  $i = 1, \dots, N_x$ ,  $j = 1, \dots, N_y$  with  $x_{i+1/2} = x_l + i\Delta x$ ,  $y_{j+1/2} = y_l + j\Delta y$ , and  $\Delta x = \frac{x_r - x_l}{N_x}$ ,  $\Delta y = \frac{y_r - y_l}{N_y}$ . Let  $\mathbf{U}_{i,j}^n$  be the approximation of the solution  $\mathbf{U}$  on the  $(i, j)$ -th mesh cell at the  $n$ -th time step  $t_n$ .

For the purpose to validate the model, the numerical scheme for (5.1) the simpler the better that we adopt abruptly a splitting scheme in each time step. Precisely, we split it into three parts: convection terms in two spatial directions and the source term as

$$\text{convection in } x\text{-direction: } \frac{1}{c} \frac{\partial \mathbf{U}}{\partial t} + \frac{\partial \mathbf{F}_1(\mathbf{U})}{\partial x} + \mathbf{R}_1(\mathbf{U}) \frac{\partial \mathbf{U}}{\partial x} = 0, \quad (5.2)$$

$$\text{convection in } y\text{-direction: } \frac{1}{c} \frac{\partial \mathbf{U}}{\partial t} + \frac{\partial \mathbf{F}_2(\mathbf{U})}{\partial y} + \mathbf{R}_2(\mathbf{U}) \frac{\partial \mathbf{U}}{\partial y} = 0, \quad (5.3)$$

$$\text{source part: } \frac{1}{c} \frac{\partial \mathbf{U}}{\partial t} = \mathbf{S}. \quad (5.4)$$

Next, we give the numerical scheme for both parts in our code.

**Source term** The right hand side  $\mathcal{S}(I)$  denotes the actions by the background medium on the photons. Generally, it contains a scattering term, an absorption term, and an emission term, and has the form [5, 33]

$$\mathcal{S}(I) = \frac{1}{4\pi} \sigma_s \int_{\mathbb{S}^2} I \, d\mu - (\sigma_a + \sigma_s) I + \frac{1}{4\pi} \sigma_a a c T^4 + \frac{s}{4\pi}, \quad (5.5)$$

where  $a$  is the radiation constant;  $T(\mathbf{x}, t)$  is the material temperature;  $\sigma_a(\mathbf{x}, T)$ ,  $\sigma_s(\mathbf{x}, T)$  and  $\sigma_t = \sigma_a + \sigma_s$  are the absorption, scattering, and total opacity coefficients, respectively; and  $s(\mathbf{x})$  is an isotropic external source. The temperature is related to the internal energy  $e$ , whose evolution equation is

$$\frac{\partial e}{\partial t} = \sigma_a \left( \int_{\mathbb{S}^2} I \, d\Omega - a c T^4 \right). \quad (5.6)$$

The relationship between  $T$  and  $e$  is problem-dependent, and we will assign it in the numerical examples when necessary.

Noticing the quartic term  $a c \sigma_a T^4$  in  $\mathcal{S}(I)$  and the evolution equation of  $e$  (5.6), we adopt the implicit Euler scheme on them as

$$\frac{\mathbf{U}_{i,j}^{n+1} - \mathbf{U}_{i,j}^n}{c \Delta t} = \mathbf{S}_{i,j}^{n+1}, \quad \frac{e_{i,j}^{n+1} - e_{i,j}^n}{\Delta t} = \sigma_{a,i,j}^{n+1} (E_{0,i,j}^{n+1} - a c (T_{i,j}^{n+1})^4).$$

One can directly check that in the absence of any external source of radiation, i.e.,  $s = 0$ , this discretization satisfies the conservation of total energy as

$$\frac{e_{i,j}^{n+1} - e_{i,j}^n}{\Delta t} + \frac{E_{0,i,j}^{n+1} - E_{0,i,j}^n}{c \Delta t} = 0.$$

**Convection part** Without loss of generality, we only consider the convection part in  $x$ -direction. For a better reading experience below, the subscript of dimension is suppressed, i.e. we will use  $\mathbf{F}$  and  $\mathbf{R}$  instead of  $\mathbf{F}_1$  and  $\mathbf{R}_1$ . The hyperbolic regularization in Section 4 modifies the governing equation of  $E_\alpha$ ,  $\alpha \in \mathcal{I}_N$ ,  $|\alpha| = N$ , such that these equations can not be written into a conservation form. Therefore, the classical Riemann solvers for hyperbolic conservation laws can not be directly applied to solve (5.2). In the numerical simulations of the  $HMP_N$  system in slab geometry [19], we adopt the DLM theory [32] to deal with the non-conservation terms, and we continue to use this method here. Precisely, the key is introducing a path  $\Gamma(\tau; \cdot, \cdot)$ ,  $\tau \in [0, 1]$  to connect two states  $\mathbf{U}^L$  and  $\mathbf{U}^R$  beside the Riemann problem such that

$$\Gamma(0; \mathbf{U}^L, \mathbf{U}^R) = \mathbf{U}^L, \quad \Gamma(1; \mathbf{U}^L, \mathbf{U}^R) = \mathbf{U}^R.$$

The path allows a generalization of the Rankine-Hugoniot condition to the non-conservation system as

$$\mathbf{F}(\mathbf{U}^L) - \mathbf{F}(\mathbf{U}^R) + \int_0^1 [v_s \mathbf{I} - \mathbf{R}(\Gamma(\tau; \mathbf{U}^L, \mathbf{U}^R))] \frac{\partial \Gamma}{\partial \tau}(\tau; \mathbf{U}^L, \mathbf{U}^R) \, d\tau = 0, \quad (5.7)$$

if the two states  $\mathbf{U}^L$  and  $\mathbf{U}^R$  are connected by a shock with shock speed  $v_s$ . Then the weak solution of the non-conservation system can be defined. Readers can find more details of the constrained path



and the theory results in [32]. We then introduce the finite volume scheme in [38] to discretize the non-conservation system (5.2). This scheme can be treated as a non-conservation version of the HLL scheme and has been successfully applied to some non-conservation models [12, 11].

Applying the finite volume scheme in [38] yields

$$\frac{U_{i,j}^{n+1} - U_{i,j}^n}{c\Delta t} + \frac{\hat{\mathbf{F}}_{i+1/2,j}^n - \hat{\mathbf{F}}_{i-1/2,j}^n}{\Delta x} + \frac{\hat{\mathbf{R}}_{i+1/2,j}^{n-} - \hat{\mathbf{R}}_{i-1/2,j}^{n+}}{\Delta x} = 0. \quad (5.8)$$

Here the flux  $\hat{\mathbf{F}}_{i+1/2,j}^n$  is the HLL numerical flux for the conservation term  $\frac{\partial \mathbf{F}(\mathbf{U})}{\partial x}$ , given by

$$\hat{\mathbf{F}}_{i+1/2,j}^n = \begin{cases} \mathbf{F}(\mathbf{U}_{i,j}^n), & \lambda_{i+1/2,j}^L \geq 0, \\ \frac{\lambda_{i+1/2,j}^R \mathbf{F}(\mathbf{U}_{i,j}^n) - \lambda_{i+1/2,j}^L \mathbf{F}(\mathbf{U}_{i+1,j}^n) + \lambda_{i+1/2,j}^L \lambda_{i+1/2,j}^R (\mathbf{U}_{i+1,j}^n - \mathbf{U}_{i,j}^n)}{\lambda_{i+1/2,j}^R - \lambda_{i+1/2,j}^L}, & \lambda_{i+1/2,j}^L < 0 < \lambda_{i+1/2,j}^R, \\ \mathbf{F}(\mathbf{U}_{i+1,j}^n), & \lambda_{i+1/2,j}^R \leq 0, \end{cases} \quad (5.9)$$

where  $\lambda_{i+1/2,j}^L$  and  $\lambda_{i+1/2,j}^R$  are defined as

$$\lambda_{i+1/2,j}^L = \min(\lambda_{i,j}^L, \lambda_{i+1,j}^L), \quad \lambda_{i+1/2,j}^R = \max(\lambda_{i,j}^R, \lambda_{i+1,j}^R).$$

Here  $\lambda_{i,j}^L$  and  $\lambda_{i,j}^R$  are the minimum and maximum characteristic speeds of  $\mathbf{U}_{i,j}^n$ , respectively. flux  $\hat{\mathbf{R}}_{i+1/2,j}^{n\pm}$  is the special treatment of the finite volume scheme in [38] for the non-conservation term  $\mathbf{R}(\mathbf{U}) \frac{\partial \mathbf{U}}{\partial x}$ , given by

$$\hat{\mathbf{R}}_{i+1/2,j}^{n-} = \begin{cases} 0, & \lambda_{i+1/2,j}^L \geq 0, \\ -\frac{\lambda_{i+1/2,j}^L \mathbf{g}_{i+1/2,j}^n}{\lambda_{i+1/2,j}^R - \lambda_{i+1/2,j}^L}, & \lambda_{i+1/2,j}^L < 0 < \lambda_{i+1/2,j}^R, \\ \mathbf{g}_{i+1/2,j}^n, & \lambda_{i+1/2,j}^R \leq 0, \end{cases} \quad (5.10)$$

and

$$\hat{\mathbf{R}}_{i+1/2,j}^{n+} = \begin{cases} -\mathbf{g}_{i+1/2,j}^n, & \lambda_{i+1/2,j}^L \geq 0, \\ -\frac{\lambda_{i+1/2,j}^R \mathbf{g}_{i+1/2,j}^n}{\lambda_{i+1/2,j}^R - \lambda_{i+1/2,j}^L}, & \lambda_{i+1/2,j}^L < 0 < \lambda_{i+1/2,j}^R, \\ 0, & \lambda_{i+1/2,j}^R \leq 0, \end{cases} \quad (5.11)$$

where

$$\mathbf{g}_{i+1/2,j}^n = \int_0^1 \mathbf{R}(\Gamma(\tau; \mathbf{U}_{i,j}^n, \mathbf{U}_{i+1,j}^n)) \frac{\partial \Gamma}{\partial \tau}(\tau; \mathbf{U}_{i,j}^n, \mathbf{U}_{i+1,j}^n) d\tau. \quad (5.12)$$

Since the implicit scheme is adopted in the discretization of the source term, one can easily check that the discretization is unconditionally stable. Thus the time step is constrained by the convection term and complies with the CFL condition

$$\text{CFL} := \max_{i,j} |\lambda(\mathbf{U}_{i,j}^n)| \frac{\Delta t}{\Delta x} < 1.$$

Notice  $\mathbf{w}$  and  $\mathbf{U}$  are uniquely determined by each other, therefore the path  $\Gamma(\tau; \mathbf{U}^L, \mathbf{U}^R)$  is equivalent to the path  $\gamma(\tau; \mathbf{w}^L, \mathbf{w}^R)$ , where  $\mathbf{w}$  is defined in (4.10), and  $\mathbf{w}^L$  and  $\mathbf{w}^R$  are the value of  $\mathbf{w}$  when  $\mathbf{U}$  is equal to  $\mathbf{U}^L$  and  $\mathbf{U}^R$ , respectively. In [19], we verified that the choice of the path  $\Gamma(\tau; \cdot, \cdot)$  is not essential, thus in this paper we simply choose the path as a linear path between  $\mathbf{w}^L$  and  $\mathbf{w}^R$ , i.e.

$$\gamma(\tau; \mathbf{w}^L, \mathbf{w}^R) = \mathbf{w}^L + \tau(\mathbf{w}^R - \mathbf{w}^L), \quad 0 \leq \tau \leq 1.$$

**Boundary condition** We adopt the method in [20] and [19] to deal with the boundary condition. In Section 3, one can determine an injective function between the distribution function  $\hat{f}$  and the moments  $E_\alpha$ , thus we can construct the boundary condition of the reduced model based on the boundary condition of the RTE. Without loss of generality, we take the left boundary, i.e.  $x = x_l$  and  $i = 0$  in  $U_{i,j}$  as an example.

On the left boundary, the specific intensity is given by

$$I^B(t, \mathbf{x}; \boldsymbol{\Omega}) = \begin{cases} I(t, \mathbf{x}; \boldsymbol{\Omega}), & \boldsymbol{\Omega} \cdot \mathbf{e}_x < 0, \\ I_{\text{out}}(t, \mathbf{x}; \boldsymbol{\Omega}), & \boldsymbol{\Omega} \cdot \mathbf{e}_x > 0, \end{cases}$$

where  $I_{\text{out}}$  is the specific intensity outside of the domain, which depends on the specific problem and the intensity inside the domain on the boundary  $I(t, \mathbf{x}; \boldsymbol{\Omega})$ , where  $\mathbf{x}_1 = x_l$ . Here we list some of the commonly used boundary conditions and the choices of the intensity  $I_{\text{out}}$ , for later usage.

- Infinite boundary condition:

$$I_{\text{out}}(t, \mathbf{x}; \boldsymbol{\Omega}) = I(t, \mathbf{x}; \boldsymbol{\Omega}), \quad \boldsymbol{\Omega} \cdot \mathbf{e}_x > 0.$$

- Reflective boundary condition:

$$I_{\text{out}}(t, \mathbf{x}; \boldsymbol{\Omega}) = I(t, \mathbf{x}; \boldsymbol{\Omega} - 2(\boldsymbol{\Omega} \cdot \mathbf{e}_x)\mathbf{e}_x), \quad \boldsymbol{\Omega} \cdot \mathbf{e}_x > 0.$$

- Vacuum boundary condition:

$$I_{\text{out}}(t, \mathbf{x}; \boldsymbol{\Omega}) = 0, \quad \boldsymbol{\Omega} \cdot \mathbf{e}_x > 0.$$

- Inflow boundary condition:

$$I_{\text{out}}(t, \mathbf{x}; \boldsymbol{\Omega}) = I_{\text{inflow}}(t, \mathbf{x}; \boldsymbol{\Omega}), \quad \boldsymbol{\Omega} \cdot \mathbf{e}_x > 0.$$

where  $I_{\text{inflow}}$  is the specific intensity of the external inflow.

Furthermore, we replace the intensity  $I(t, \mathbf{x}; \boldsymbol{\Omega})$  by the specific intensity constructed by the moments in the cell near the left boundary. Precisely,

$$I(t, \mathbf{x}; \boldsymbol{\Omega}) = \hat{I}(\boldsymbol{\Omega}; U(t, \mathbf{x})),$$

where  $U(t, \mathbf{x})$  is the moments in the cell near the left boundary, i.e.  $[x_{1/2} = x_l, x_{3/2} = x_l + \Delta x] \times [y_{j-1/2}, y_{j+1/2}]$  at time  $t$ . Then one can directly obtain the flux across the left boundary. Precisely, the  $\alpha$ -th flux at  $t$  and  $\mathbf{x}$  is given by

$$\int_{\mathbb{S}^2} \boldsymbol{\Omega}^{\alpha+e_1} I^B(t, \mathbf{x}; \boldsymbol{\Omega}) d\boldsymbol{\Omega} = \int_{\boldsymbol{\Omega} \cdot \mathbf{e}_x < 0} \boldsymbol{\Omega}^{\alpha+e_1} \hat{I}(\boldsymbol{\Omega}; U(t, \mathbf{x})) d\boldsymbol{\Omega} + \int_{\boldsymbol{\Omega} \cdot \mathbf{e}_x > 0} \boldsymbol{\Omega}^{\alpha+e_1} I_{\text{out}}(t, \mathbf{x}; \boldsymbol{\Omega}) d\boldsymbol{\Omega}.$$

## 5.2 Numerical examples

Below, we present some numerical examples to show different features of the 3D  $HMP_N$  model.

**Inflow problem** This example is used to study the behaviour of the solution of the  $HMP_N$  model, hence the right hand side vanishes, i.e. the RTE degenerates into

$$\frac{1}{c} \frac{\partial I}{\partial t} + \boldsymbol{\Omega} \cdot \nabla_{\mathbf{x}} I = 0. \quad (5.13)$$

The initial state is chosen as

$$I_0(\mathbf{x}; \boldsymbol{\Omega}) = \begin{cases} ac\delta(\boldsymbol{\Omega} - \boldsymbol{\Omega}_0), & x < 0 \text{ and } y < 0, \\ \frac{10^{-3}}{4\pi} ac, & \text{otherwise,} \end{cases}$$

where  $\|\boldsymbol{\Omega}_0\| = 1$ . The distribution function is a Dirac delta function, which is extremely anisotropic and hard to approximate with the  $P_N$  model, which approximates the specific intensity with polynomials. On the other hand, due to the fact the  $S_N$  model only considers the particles along with a discrete set of angular directions, when the  $\boldsymbol{\Omega}_0$  does not belong to this set, the  $S_N$  model can not get a good approximation.

The computational domain is  $[-0.2, 0.2] \times [-0.2, 0.2]$ , and the infinite boundary conditions are prescribed at the boundaries.

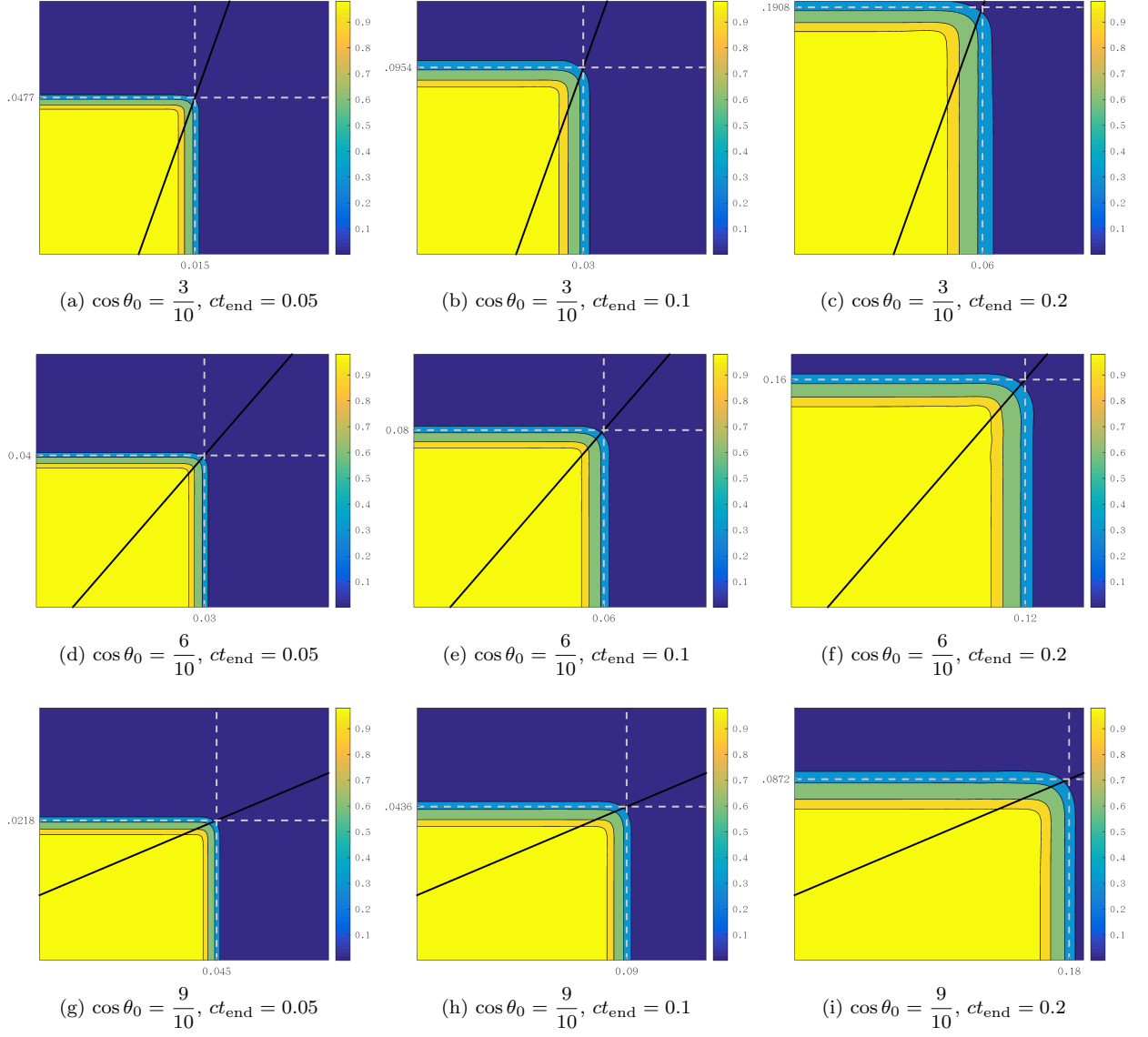


Figure 1: Profile of  $E_0$  of the inflow problem with the  $HMP_2$  model, where the directions are different

In order to validate the capability of the 3D  $HMP_N$  model to simulate Dirac delta functions in any direction, we choose some different  $\mathbf{\Omega}_0$ , with  $\mathbf{\Omega}_0 = (\cos \theta_0, \sin \theta_0)$ , and  $\cos \theta_0 = \frac{3}{10}, \frac{6}{10}$ , and  $\frac{9}{10}$ . We simulate this problem with the 3D  $HMP_N$  model till  $ct_{\text{end}} = 0.05, 0.1$ , and  $0.2$ , with  $N = 2$ .  $N_x = N_y = 160$  is applied in this example. The results of the contours of  $\frac{E_0}{ac}$  are presented in Figure 1. The black line represents the direction of  $\mathbf{\Omega}_0$ , i.e. the slope of each line is  $\tan \theta_0$ , and the dashed lines ( $x = ct_{\text{end}} \cos \theta_0$  and  $y = ct_{\text{end}} \sin \theta_0$ ) figure out the theoretical results of the wave in  $x$ -direction and  $y$ -direction, respectively. From the results, one can conclude that the 3D  $HMP_N$  model can capture the wave well. Therefore, the approximation of the  $HMP_N$  to the delta function in any direction is satisfying.

**Gaussian source problem** This example is to show the rotational invariance of the  $MP_N$  model. The initial specific intensity is a Gaussian distribution in space [23]:

$$I_0(\mathbf{x}; \mathbf{\Omega}) = \frac{1}{4\pi} \frac{ac}{\sqrt{2\pi}\theta} e^{-\frac{\|\mathbf{x}\|^2}{2\theta^2}}, \quad \theta = \frac{1}{100}, \quad \mathbf{x} \in (-L, L) \times (-L, L). \quad (5.14)$$

Here the computational domain is set by  $L = 1$ , and  $ct_{\text{end}} = 0.5$  so that that the energy reaching the boundaries is negligible, and vacuum boundary conditions are prescribed at all the boundaries. The medium is purely scattering with  $\sigma_s = \sigma_t = 1$ , thus the material coupling term vanishes. We also set the external source to be zero.

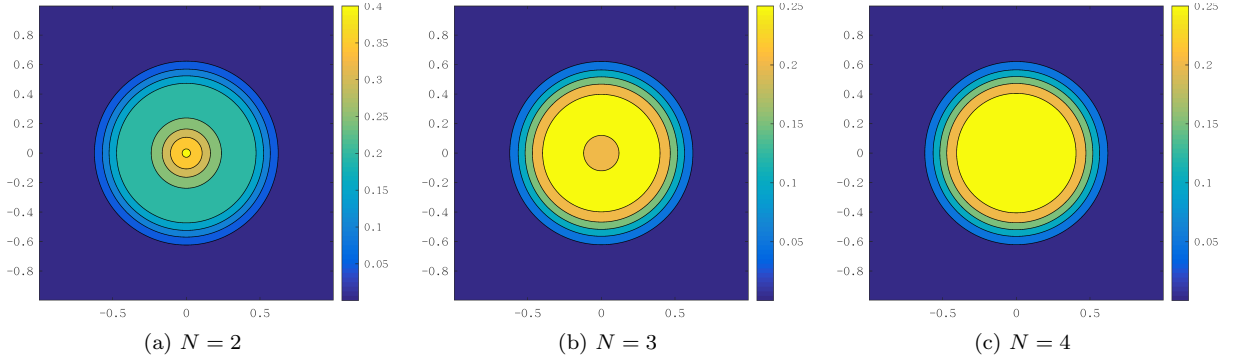


Figure 2: Profile of  $E_0$  of the Gaussian source problem with the  $HMP_N$  model

We use  $400 \times 400$  cells to simulate this problem, with the  $HMP_2$  model, the  $HMP_3$  model, and the  $HMP_4$  model, and the results are presented in Figure 2, from which one can conclude the contours of the  $\frac{E_0}{ac}$  are circles and there is no ray effect. This validates the rotational invariance of the 3D  $HMP_N$  model.

**Bilateral inflow problem** In the previous numerical example, we validate the capability of the 3D  $HMP_N$  model to simulate Dirac delta function. In this example, we show that the 3D  $HMP_N$  model can also approximate isotropic distribution function.

We use the RTE without right hand side (5.13), and the initial state is chosen as

$$I_0(\mathbf{x}; \mathbf{\Omega}) = \begin{cases} ac\delta(\mathbf{\Omega} - \mathbf{\Omega}_0), & x < -\frac{2}{10} \text{ and } y < -\frac{2}{10}, \\ \frac{ac}{4\pi}, & x > \frac{2}{10} \text{ and } y > \frac{2}{10}, \\ \frac{10^{-3}}{4\pi}ac, & \text{otherwise,} \end{cases}$$

where  $\mathbf{\Omega}_0 = (\frac{\sqrt{2}}{2}, \frac{\sqrt{2}}{2})^T$ . In the bottom-left region, the distribution function is a Dirac delta function, which is extremely anisotropic and hard to approximate with the  $P_N$  model, which approximates the specific intensity with polynomials. Meanwhile, in the upper-right region, the distribution function is a constant with respect to the velocity direction  $\mathbf{\Omega}$ , which is isotropic. Generally, it is challenging to get a good approximation on a Dirac delta function and a constant function.

The computational domain is  $[-1, 1] \times [-1, 1]$ , and the infinite boundary conditions are prescribed at the boundaries. We simulate this problem with the  $HMP_N$  model and the  $P_N$  model till  $ct_{\text{end}} = 0.1$  with  $N = 2, 3$ , and 4.  $N_x = N_y = 400$  is applied in this example.

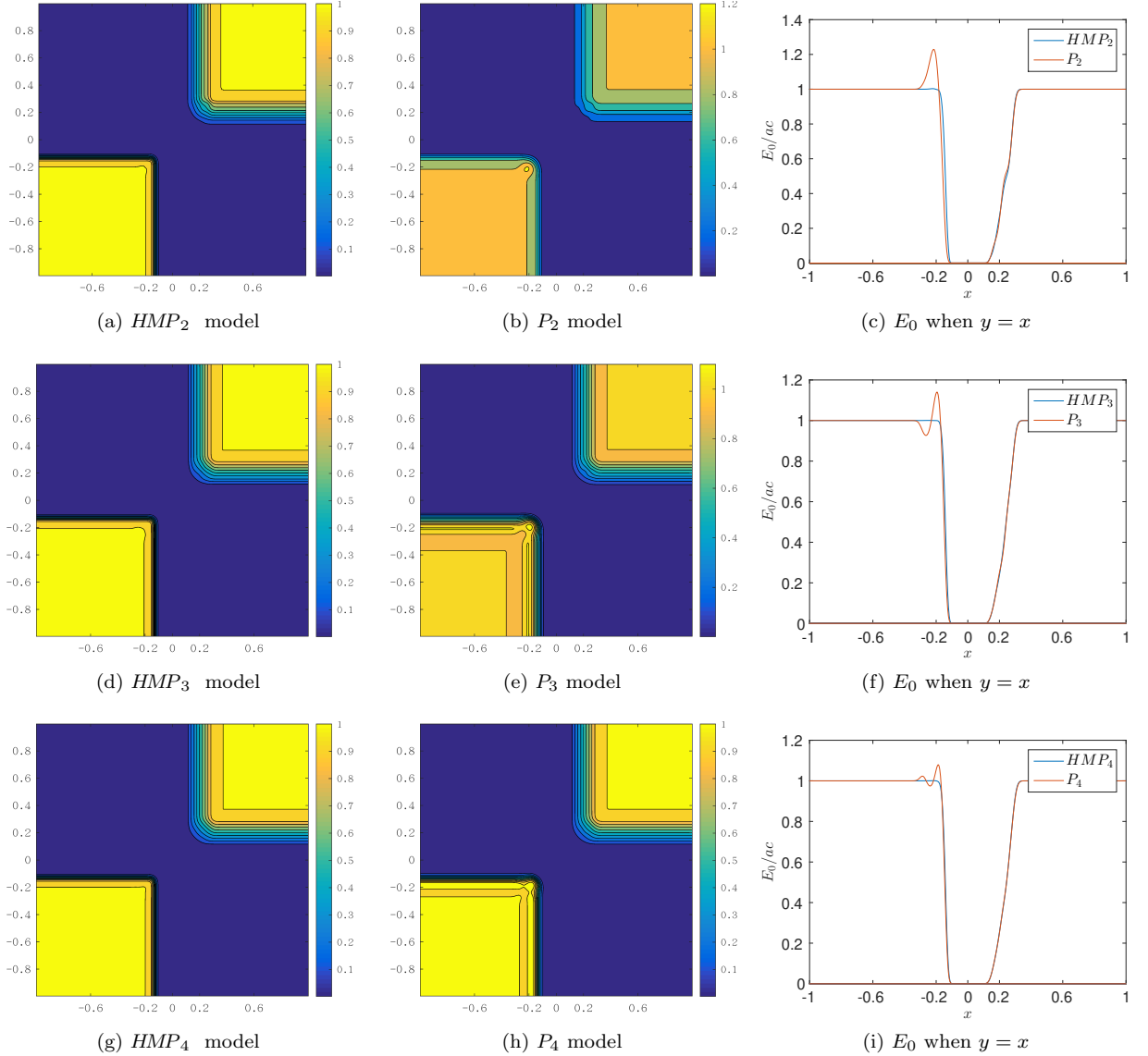


Figure 3: Profile of  $E_0$  of the bilateral inflow with the  $HMP_2$  model and the  $P_2$  model

In Figure 3, we present the  $E_0$  of the 3D  $HMP_N$  model and the  $P_N$  model for  $N = 2, 3$ , and 4, and additionally, we present the  $\frac{E_0}{ac}$  of these two models along the line  $y = x$ . According to the results in Figure 3, we can conclude that in the upper-right region, for this constant function, the  $HMP_N$  model and the  $P_N$  model gets similar results, i.e. these two models can approximate this kind of isotropic function well. However, in the bottom-left region, for this Dirac delta function, the  $HMP_N$  model gets a good approximation, but there are unphysical oscillations in the results of the  $P_N$  model. In particular, due to these unphysical oscillations, along the line  $y = x$ ,  $\frac{E_0}{ac}$  of the  $P_N$  model can be even greater than 1. Therefore, one can conclude that the  $HMP_N$  model can not only get a good approximate on an isotropic distribution function, but also approximate the Dirac delta function well.

**Lattice problem** The lattice problem is a checkerboard of highly scattering and highly absorbing regions loosely based on a small part of a lattice core. The computational domain is  $[0, 7] \times [0, 7]$ , divided into 49 grids in Figure 4. In the red grids and the black grid, the absorbing and scattering coefficients are 0 and 1 respectively. In the white grids, the absorption and scattering are 10 and 0, respectively. The

external source  $s$  is set as  $ac$  in the black grid, and 0 in other grids. The initial state is set as  $I = 10^{-8}ac$ , and vacuum boundary condition are prescribed on all boundaries.

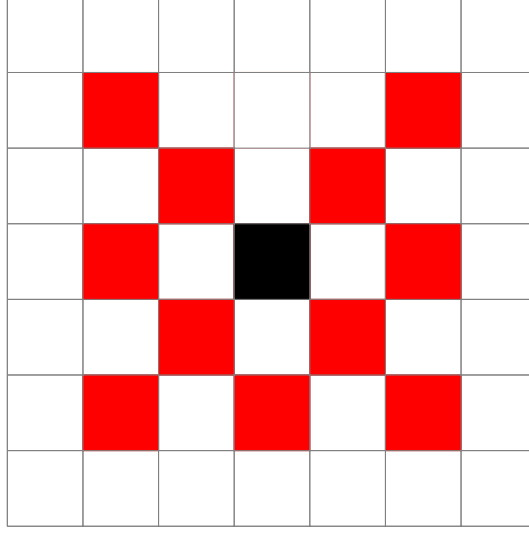


Figure 4: Computational domain of the lattice problem

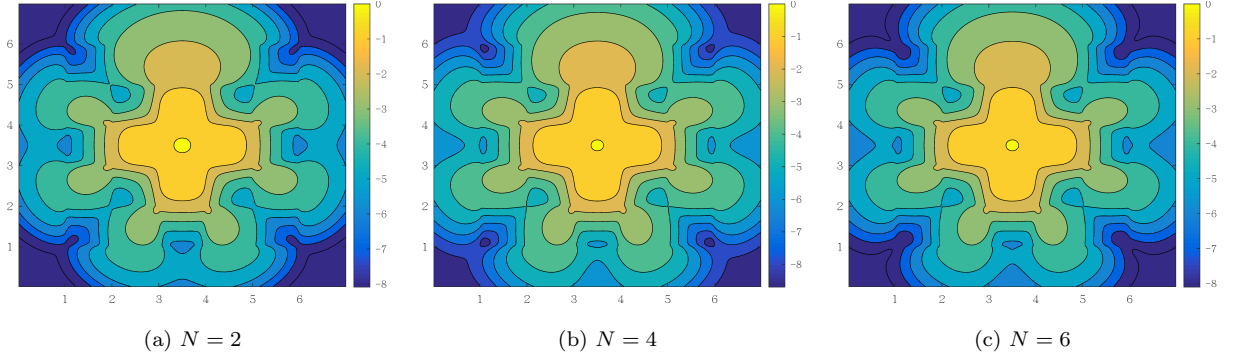


Figure 5: Profile of  $E_0$  of the lattice problem with the  $HMP_N$  model

We simulate this problem with the  $HMP_N$  model with  $N = 2, 4$ , and 6 till  $ct_{\text{end}} = 3.2$ , the number of grids is  $200 \times 200$ , and the results of  $\log_{10} \frac{E_0}{ac}$  are presented in Figure 5. According to the results, the  $HMP_N$  model gives a satisfying result, and the result of  $E_0$  is always positive in this problem.

## 6 Conclusion

The 3D  $HMP_N$  model was derived as a reduced nonlinear model for RTE in 3D space. The model is hopeful to capture both very singular specific intensity as Dirac delta function and very regular specific intensity as constant function. The model has some mathematical advantages, including global hyperbolicity, rotational invariance, physical wave speeds, spectral accuracy, and correct higher-order Eddington approximation. We validated the new model by some preliminary numerical results. In the following, we will try to apply the model to some practical problems.

## Acknowledgements

The authors are partially supported by Science Challenge Project, No. TZ2016002, the CAEP foundation (No. CX20200026), and the National Natural Science Foundation of China (Grant No. 91630310 and 11421110001, 11421101).

## References

- [1] E. Abdikamalov, A. Burrows, C. D. Ott, F. Löffler, E. O'Connor, J. C. Dolence, and E. Schnetter. A new Monte Carlo method for time-dependent neutrino radiation transport. *The Astrophysical Journal*, 755(2):111, 2012.
- [2] G. W. Alldredge, R. Li, and W. Li. Approximating the  $M_2$  method by the extended quadrature method of moments for radiative transfer in slab geometry. *Kinetic & Related Models*, 9(2), 2016.
- [3] G. Bird. *Molecular Gas Dynamics and the Direct Simulation of Gas Flows*. Oxford: Clarendon Press, 1994.
- [4] J. E. Broadwell. Study of rarefied shear flow by the discrete velocity method. *Journal of Fluid Mechanics*, 19(03):401–414, 1964.
- [5] T. A. Brunner. Forms of approximate radiation transport. *Tech. Rep SAND2002-1778*, 2002.
- [6] T. A. Brunner and J. P. Holloway. One-dimensional Riemann solvers and the maximum entropy closure. *Journal of Quantitative Spectroscopy and Radiative Transfer*, 69(5):543–566, 2001.
- [7] T. A. Brunner and J. P. Holloway. Two-dimensional time dependent Riemann solvers for neutron transport. *Journal of Computational Physics*, 210:386–399, 2005.
- [8] Z. Cai, Y. Fan, and R. Li. Globally hyperbolic regularization of Grad's moment system in one dimensional space. *Comm. Math. Sci.*, 11(2):547–571, 2013.
- [9] Z. Cai, Y. Fan, and R. Li. Globally hyperbolic regularization of Grad's moment system. *Comm. Pure Appl. Math.*, 67(3):464–518, 2014.
- [10] Z. Cai, Y. Fan, and R. Li. A framework on moment model reduction for kinetic equation. *SIAM J. Appl. Math.*, 75(5):2001–2023, 2015.
- [11] Z. Cai, Y. Fan, R. Li, and Z. Qiao. Dimension-reduced hyperbolic moment method for the Boltzmann equation with BGK-type collision. *Commun. Comput. Phys.*, 15(5):1368–1406, 2014.
- [12] Z. Cai, R. Li, and Z. Qiao. Globally hyperbolic regularized moment method with applications to microflow simulation. *Computers and Fluids*, 81:95–109, 2013.
- [13] B. Davison. On the rate of convergence of the spherical harmonics method for the plane case, isotropic scattering. *Canadian Journal of Physics*, 38(11):1526–1545, 1960.
- [14] J. D. Densmore, K. G. Thompson, and T. J. Urbatsch. A hybrid transport-diffusion Monte Carlo method for frequency-dependent radiative-transfer simulations. *Journal of Computational Physics*, 231(20):6924–6934, 2012.
- [15] B. Dubroca and J. Feugeas. Theoretical and numerical study on a moment closure hierarchy for the radiative transfer equation. *Comptes Rendus de l'Academie des Sciences Series I Mathematics*, 329(10):915–920, 1999.
- [16] J. J. Duderstadt and W. R. Martin. *Transport theory*. Wiley, New York, 1979.
- [17] Y. Fan, J. An, and L. Ying. Fast algorithms for integral formulations of steady-state radiative transfer equation. *Journal of Computational Physics*, 380:191–211, 2019.
- [18] Y. Fan, J. Koellermeier, J. Li, R. Li, and M. Torrilhon. Model reduction of kinetic equations by operator projection. *Journal of Statistical Physics*, 162(2):457–486, 2016.
- [19] Y. Fan, R. Li, and L. Zheng. A nonlinear hyperbolic model for radiative transfer equation in slab geometry. *arXiv preprint arXiv:1911.05472*, 2019.
- [20] Y. Fan, R. Li, and L. Zheng. A nonlinear moment model for radiative transfer equation in slab geometry. *Journal of Computational Physics*, 404:109128, 2020.
- [21] J. Fleck and J. Cummings. An implicit Monte Carlo scheme for calculating time and frequency dependent nonlinear radiation transport. *J. Comput. Phys.*, 8(3):313–342, 1971.

- [22] C. Hauck and R. McClarren. Positive  $P_N$  closures. *SIAM Journal on Scientific Computing*, 32(5):2603–2626, 2010.
- [23] C. D. Hauck, M. Frank, and E. Olbrant. Perturbed, entropy-based closure for radiative transfer. *SIAM Journal on Applied Mathematics*, 6(3):557–587, 2013.
- [24] C. K. Hayakawa, J. Spanier, and V. Venugopalan. Coupled forward-adjoint Monte Carlo simulations of radiative transport for the study of optical probe design in heterogeneous tissues. *SIAM Journal on Applied Mathematics*, 68(1):253–270, 2007.
- [25] J. H. Jeans. Stars, gaseous, radiative transfer of energy. *Monthly Notices of the Royal Astronomical Society*, 78:28–36, 1917.
- [26] A. D. Klose, U. Netz, J. Beuthan, and A. H. Hielscher. Optical tomography using the time-independent equation of radiative transfer part 1: forward model. *Journal of Quantitative Spectroscopy and Radiative Transfer*, 72(5):691–713, 2002.
- [27] R. Koch and R. Becker. Evaluation of quadrature schemes for the discrete ordinates method. *Journal of Quantitative Spectroscopy and Radiative Transfer*, 84(4):423–435, 2004.
- [28] E. W. Larsen and J. E. Morel. Advances in discrete-ordinates methodology. In *Nuclear Computational Science*, pages 1–84. Springer, 2010.
- [29] C. D. Levermore. Moment closure hierarchies for kinetic theories. *Journal of Statistical Physics*, 83(5-6):1021–1065, 1996.
- [30] R. Li, W. Li, and L. Zheng. A nonlinear three-moment model for radiative transfer in spherical symmetry. *Mathematics and Computers in Simulation*, 170:285 – 299, 2020.
- [31] A. Marshak and A. Davis. *3D radiative transfer in cloudy atmospheres*. Springer Science & Business Media, 2005.
- [32] G. D. Maso, P. G. LeFloch, and F. Murat. Definition and weak stability of nonconservative products. *J. Math. Pures Appl.*, 74(6):483–548, 1995.
- [33] R. G. McClarren, T. M. Evans, R. B. Lowrie, and J. D. Densmore. Semi-implicit time integration for  $P_N$  thermal radiative transfer. *Journal of Computational Physics*, 227(16):7561–7586, 2008.
- [34] R. G. McClarren, J. P. Holloway, and T. A. Brunner. On solutions to the  $P_n$  equations for thermal radiative transfer. *Journal of Computational Physics*, 227(5):2864–2885, 2008.
- [35] D. Mihalas. *Stellar Atmospheres*. San Francisco, WH Freeman and Co., 650p, 1978.
- [36] G. N. Minerbo. Maximum entropy eddington factors. *Journal of Quantitative Spectroscopy and Radiative Transfer*, 20(6):541–545, 1978.
- [37] G. Pomraning. *The equations of radiation hydrodynamics*. Pergamon Press, 1973.
- [38] S. Rhebergen, O. Bokhove, and J. J. W. van der Vegt. Discontinuous Galerkin finite element methods for hyperbolic nonconservative partial differential equations. *J. Comput. Phys.*, 227(3):1887–1922, 2008.
- [39] K. Stamnes, S.-C. Tsay, W. Wiscombe, and K. Jayaweera. Numerically stable algorithm for discrete-ordinate-method radiative transfer in multiple scattering and emitting layered media. *Appl. Opt.*, 27(12):2502–2509, Jun 1988.
- [40] T. Tarvainen, M. Vauhkonen, V. Kolehmainen, and J. P. Kaipio. Hybrid radiative-transfer–diffusion model for optical tomography. *Applied optics*, 44(6):876–886, 2005.